



Published in final edited form as:

Cell Rep. 2022 December 13; 41(11): 111800. doi:10.1016/j.celrep.2022.111800.

## Hypoxia induces transgenerational epigenetic inheritance of small RNAs

Simon Yuan Wang<sup>1,2,\*</sup>, Kathleen Kim<sup>2,4</sup>, Zach Klapholz O’Brown<sup>1,2,4</sup>, Aileen Levan<sup>2</sup>, Anne Elizabeth Dodson<sup>3</sup>, Scott G. Kennedy<sup>3</sup>, Chaim Chernoff<sup>1,2</sup>, Eric Lieberman Greer<sup>1,2,5,\*</sup>

<sup>1</sup>Department of Pediatrics, HMS Initiative for RNA Medicine, Harvard Medical School, Boston, MA 02115, USA

<sup>2</sup>Division of Newborn Medicine, Boston Children’s Hospital, Boston, MA 02115, USA

<sup>3</sup>Department of Genetics, Blavatnik Institute at Harvard Medical School, Boston, MA 02115, USA

<sup>4</sup>These authors contributed equally

<sup>5</sup>Lead contact

### SUMMARY

Animals sense and adapt to decreased oxygen availability, but whether and how hypoxia exposure in ancestors can elicit phenotypic consequences in normoxia-reared descendants are unclear. We show that hypoxia induces an intergenerational reduction in lipids and a transgenerational reduction in fertility in the nematode *Caenorhabditis elegans*. The transmission of these epigenetic phenotypes is dependent on repressive histone-modifying enzymes and the argonaute HRDE-1. Feeding naive *C. elegans* small RNAs extracted from hypoxia-treated worms is sufficient to induce a fertility defect. Furthermore, the endogenous small interfering RNA *F44E5.4/5* is upregulated intergenerationally in response to hypoxia, and soaking naive normoxia-reared *C. elegans* with *F44E5.4/5* double-stranded RNA (dsRNA) is sufficient to induce an intergenerational fertility defect. Finally, we demonstrate that labeled *F44E5.4/5* dsRNA is itself transmitted from parents to children. Our results suggest that small RNAs respond to the environment and are sufficient to transmit non-genetic information from parents to their naive children.

### In brief

This is an open access article under the CC BY-NC-ND license (<http://creativecommons.org/licenses/by-nc-nd/4.0/>).

\*Correspondence: yuan.wang@childrens.harvard.edu (S.Y.W.), eric.greer@childrens.harvard.edu (E.L.G.).

#### AUTHOR CONTRIBUTIONS

E.L.G. and S.Y.W. conceived and planned the study and wrote the paper. All authors discussed the results and commented on the manuscript. S.Y.W. performed the experiments and data analysis and produced all figures with help from the co-authors. K.K. helped produce Figures 1E, 2F, 3, 4B, 5D–5F, S1E, S1F, S2G, and S3 and was advised by S.Y.W. Z.K.O. helped conceive the study, performed some of the initial phenotypic characterizations of the transgenerational hypoxia response, and helped produce Figures 1E and 3A. A.L. helped produce Figures 1C–1E, 3B, and 3F and was advised by S.Y.W. A.E.D. generated the *hrde-1::GFP* strain and was advised by S.G.K. C.C. helped produce Figure 1E and was advised by S.Y.W. E.L.G. produced Figures 1B and S5I.

#### DECLARATION OF INTERESTS

The authors declare no competing interests.

#### INCLUSION AND DIVERSITY

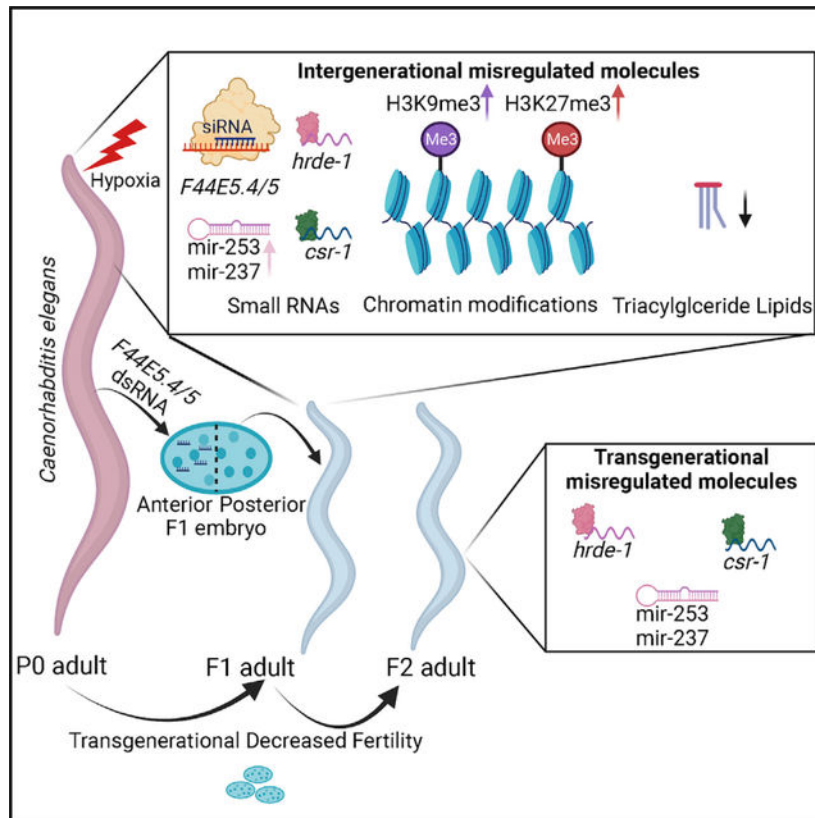
We support inclusive, diverse, and equitable conduct of research.

#### SUPPLEMENTAL INFORMATION

Supplemental information can be found online at <https://doi.org/10.1016/j.celrep.2022.111800>.

Wang et al. find that hypoxia induces epigenetic inheritance of reduced lipids and fertility in worms and that this is dependent on small RNAs and repressive chromatin modifications. They show that small RNAs are sufficient to induce heritable fertility reductions and track a labeled endogenous dsRNA across generations.

## Graphical Abstract



## INTRODUCTION

Most biological traits are inherited in a Mendelian fashion through genomic DNA.<sup>2</sup> However, recent findings demonstrate that a variety of phenotypes are regulated by inherited information not encoded in DNA sequence in prokaryotes<sup>3,4</sup> and eukaryotes.<sup>5–8</sup> These non-Mendelian phenomena arise in naive wild-type (WT) descendants who have never been exposed to the environmental manipulations themselves. The inherited epigenetic information allows organisms to adapt to extreme environments and to survive under adverse conditions rapidly without mutating their genome.<sup>9</sup> The molecular mechanisms for non-genetic inheritance include DNA methylation, chemical modifications to chromatin, non-coding RNAs, microbiota, and prions.<sup>10–12</sup> In *Caenorhabditis elegans*, the inheritance of small RNAs has been implicated in regulating transgenerational gene expression in instances of antiviral protection,<sup>13</sup> starvation,<sup>14</sup> avoidance from pathogenic bacteria,<sup>15–17</sup> and stress.<sup>18</sup> These transgenerational phenotypes require RNA-binding proteins, such as the argonautes heritable RNAi-deficient 1 (HRDE-1)<sup>19</sup> and chromosome segregation and

RNAi-deficient argonaute (CSR-1),<sup>20,21</sup> to inherit small RNAs in *C. elegans* and Ago1<sup>22</sup> in *Schizosaccharomyces pombe*. Interestingly, these argonautes interact with the chromatin modification machinery to reinforce epigenetic signatures in *S. pombe*,<sup>22</sup> *C. elegans*,<sup>19,23–26</sup> *A. thaliana*,<sup>27</sup> *D. melanogaster*,<sup>28</sup> and humans.<sup>29</sup> For example, the putative histone methyltransferases *set-25* and *met-2* are involved in RNA interference (RNAi)-directed H3K9me3.<sup>30,31</sup> Similarly, a non-canonical heterochromatin mark H3K23me3 is induced by RNAi and is dependent on both *set-32* and *hrde-1*.<sup>32</sup> These, and other studies, have revealed that a confluence of multiple mechanisms functions in combination to reinforce epigenetic states and facilitate the faithful transmission of non-genetic information to naive descendants to regulate transgenerationally inherited phenotypes.

Hypoxia poses threats to organisms in various contexts. The hypoxia tumor microenvironment is associated with an increased risk of metastasis and mortality.<sup>33</sup> Intrauterine hypoxia caused by obesity, stress, nutritional deficiencies, and smoking leads to congenital disabilities and early infant death.<sup>34,35</sup> Recent studies suggest that epigenetics plays a vital role in the cellular and molecular responses to hypoxia.<sup>36</sup> The histone lysine demethylase KDM6A directly senses oxygen and elevates H3K27me3 level in hypoxic mammalian cells to block cellular differentiation and control cell fate.<sup>37</sup> Climate-change-induced hypoxia in the aquatic environment causes transgenerational impairments in fish reproduction, jeopardizing the sustainability of fish populations and biodiversity.<sup>38,39</sup> However, the mechanisms by which hypoxia initiates phenotypic changes in the parental generation that are maintained across generations and how this non-genetic information is transmitted to naive descendants are entirely unclear.

To determine how epigenetic information is transmitted from ancestors to their descendants in response to hypoxia, we developed a hypoxia paradigm in *C. elegans*. Here, we demonstrate that hypoxia induces intergenerational lipid reduction and transgenerational fertility defects in *C. elegans*. We find that the transmission of these epigenetic phenotypes is mediated by both repressive histone marks (H3K9me3 and H3K27me3) and small RNAs. We identified specific small RNAs, including the endogenous small interfering RNA (siRNA) *F44E5.4/5*, that are intergenerationally upregulated in response to ancestral hypoxia treatment. Excitingly, feeding naive *C. elegans* with small RNAs extracted from hypoxia-treated worms or feeding them with exogenous *F44E5.4/5* double-stranded RNAs (dsRNAs) was sufficient to induce heritable decreases in fertility. Finally, we demonstrated that cyanine-3 (Cy3)-labeled *F44E5.4/5* dsRNA is itself transmitted from parents to progeny. Our results demonstrate that small RNAs respond to environmental oxygen to help regulate gene expression and are necessary and sufficient to transmit non-genetic information from parents to their naive offspring.

## RESULTS

### Hypoxia induces a heritable lipid and fertility reduction

Hypoxia exposure promotes longevity, reduces lipid content, and reduces fertility in *C. elegans*.<sup>40–42</sup> To test whether hypoxia could induce heritable phenotypes, we exposed larval stage L4 worms to 0.1% oxygen for 16 h before returning to and maintaining the nematodes in normoxic oxygen (21%) (Figure 1A). Consistent with previous work,<sup>40</sup> we

found that hypoxia extends *C. elegans* lifespan by ~20% in the parental (P0) generation; however, parental hypoxia failed to extend the lifespan of naive F1 or F2 descendants (Figure 1B; Table S1). We found that hypoxia caused a reduction in neutral lipids as assessed by oil red O staining<sup>43</sup> in both the exposed parental generation (P0) and the naive normoxia-reared F1 progeny (Figures 1C and 1D). The reduction in lipids persisted until the F2 generation, when lipid content from hypoxia-reared grandparents was indistinguishable from lipid content from normoxia-reared grandparents (Figures 1C and 1D).

Consistent with previous work,<sup>42</sup> we also found a significant reduction in fertility in response to hypoxia exposure in the P0 generation (Figure 1E). The reduced fertility persisted in the naive normoxia-reared F1 and F2 descendants of hypoxia-treated ancestors before returning to similar levels as in the normoxia-raised descendants in the F3 generation (Figure 1E). To investigate the physiological changes underlying the reduced fertility, we dissected the nematodes' gonads and quantified the number of nuclei at the pachytene and diplotene stages. We found a decrease in the number of nuclei in the *C. elegans* germlines of P0, F1, and F2 generation worms after P0 hypoxia treatment, which mirrored the reduced fertility (Figures 1F and S1A–S1D). To determine whether this phenotype was maternally or paternally inherited, we crossed hypoxia-treated hermaphrodites with normoxia males and crossed hypoxia-treated males with normoxia hermaphrodites. We found that crossing hypoxia-exposed hermaphrodites with naive males partially rescued the fertility defect phenotype (Figure S1E); in contrast, crossing hypoxia-treated males with naive hermaphrodites recapitulated the hypoxia fertility defects (Figure S1F), suggesting that the transmission of this epigenetic inheritance phenotype can occur through the paternal germline. Taken together, our results reveal that parental hypoxia exposure induces an extension in longevity only in the exposed P0 generation, an intergenerational reduction in lipids in the P0 and F1 generations, and a transgenerational fertility defect in the P0, F1, and F2 generations in the nematode *C. elegans*.

### **Hypoxia induces intergenerational and transgenerational dysregulation of gene expression and chromatin modifications**

To identify what transcriptional changes underlie the phenotypic responses to hypoxia, we performed RNA sequencing (RNA-seq) in WT *C. elegans* exposed to normoxia or hypoxia, as well as in three generations of naive descendants grown in normoxic conditions at the L4 stage (P0–F3). We found 6,814 genes were dysregulated in response to hypoxia in the P0 generation (Figures 2A and 2B). Of these 6,814 genes, 2,394 genes were dysregulated intergenerationally in the naive F1 generation, and 1,067 genes were dysregulated transgenerationally in the naive F2 generation, while 279 were still dysregulated in the naive F3 generation (Figures 2A, 2B, and S2A–S2D). A comparison of the hypoxia dysregulated genes with developmentally regulated genes<sup>44</sup> suggested that differences in gene expression were not due to hypoxia affecting development (Figure S2E). An over-representation analysis (ORA) revealed that the heritably upregulated genes were enriched for genes involved in histone binding, RNA binding, and posttranscriptional gene regulation. In contrast, genes involved in oxygen binding, chemosensory behavior, and neuropeptide signaling were enriched in the heritably downregulated genes (Figures 2C and S2F). This result, in combination with previous studies on other transgenerational

epigenetic inheritance paradigms,<sup>5,13,19,25,45–48</sup> prompted us to focus on regulators of histone modifications and small RNA pathways. We found that genes involved in histone H3 lysine 4 (H3K4) methylation (*ash-2*, *set-17*, and *wdr-5.1*) and H3K9 methylation (*met-2*, *set-25*, and *set-32*) were upregulated in the P0 hypoxia-treated parents but returned to normoxia levels of expression in F1 and F2 progeny (Figure 2D). Interestingly, the H3K27me3 demethylases (*jmjd-3.1* and *jmjd-3.2*) and the small RNA argonaute *hrde-1* retained transgenerational dysregulation in gene expression through the P0, F1, and F2 generations (Figures 2D and 2E). Because gene expression of enzymes does not necessarily imply dysregulation of enzymatic function, we performed western blots for six different histone marks, including two modifications typically associated with increased chromatin accessibility (H3K4me3 and H3K4me1) and four modifications typically associated with reduced chromatin accessibility (H3K9me2, H3K9me3, H3K23me3, and H3K27me3). We found a global increase in the methylation marks for H3K4me3, H3K9me2, H3K9me3, and H3K27me3, and a non-significant trend for increased H3K4me1 and H3K23me3 in the parental P0 generation (Figures 2F, S2G, and S2H). Notably, whereas H3K4me3 largely returned to normoxia levels in the F1 generation, we found an inherited increase in H3K9 methylation and H3K27me3 (Figures 2F and S2G). All histone modifications we examined returned to normoxia levels by the F2 generation (Figures 2F, S2G, and S2H). Overall, these results demonstrate that several histone modifications are globally increased in response to hypoxia, whereas the typically repressive histone modifications H3K27me3, H3K9me2, and H3K9me3 were elevated in naive F1 intergenerationally. Interestingly, there is an upregulation of the S-adenosylmethionine (SAM) synthetase enzymes, *sams-3* and *sams-4*,<sup>49</sup> the enzymes responsible for generating the universal methyl donor SAM,<sup>50</sup> in response to hypoxia in the parental P0 generation (Figure S2I), which could help explain why histone methylation increases indiscriminately. The upregulation of SAM synthetase enzymes could synergize with the downregulation of histone demethylases and the reduction of oxygen, which is sensed by histone lysine demethylases,<sup>37,51</sup> to cause an increase in histone methylation in the P0 generation. These changes in gene expression and histone modifications, which correlate with intergenerational and transgenerational phenotypes in response to hypoxia, raise the possibility that changes in small RNAs and histone-modifying machinery could regulate the observed heritable hypoxia phenotypes.

### **Inheritance of the hypoxia-induced transgenerational fertility defect depends on the argonaute HRDE-1 and repressive chromatin-modifying enzymes**

Due to the dysregulation of epigenetic enzymes and modifications in response to ancestral hypoxia exposure (Figures 2C– 2F), we next tested whether the dysregulated enzymes were necessary for the transgenerational fertility phenotype. Therefore, we performed a directed genetic screen using *C. elegans* with mutations in critical epigenetic machinery components. We found that mutation of the H3K4 mono- and dimethyltransferases *set-17* and *set-30*,<sup>45</sup> like WT worms, displayed a three-generation persistence of reduced fertility in response to parental hypoxia, suggesting that these enzymes and H3K4me1/me2 are not required for the transgenerational fertility defect (Figures 3A and 3B). We identified six genes that are required for the initial hypoxic response in the parental generation and are therefore not compatible with examining their role in the transmission of the epigenetic phenotype. These six genes include a dsRNA transporter, *sid-1*;<sup>52</sup> the H3K23me3

methyltransferase *set-32*,<sup>32</sup> the small RNA argonautes *sago-2*<sup>53</sup> and *nrde-2*,<sup>54</sup> one of the putative H3K27me3 demethylases, *jmjd-3.1*,<sup>55</sup> and the putative methionine synthase *metr-1* (Figures 3C–3E and S3A–S3C). We also found five genes that displayed a fertility defect in the parental generation that was exposed to hypoxia but failed to transmit this reduced fertility phenotype to naive normoxia-reared F1 and F2 descendants (Figures 3F, 3G, and S3E–S3G). The genes that were necessary for the epigenetic inheritance include a small RNA argonaute *hrde-1*<sup>19</sup> (Figure 3F); the intrinsically disordered protein *meg-3*, which is involved in phase separation through RNA binding<sup>56</sup> (Figure S3E); the putative H3K9 trimethyltransferase *set-25*<sup>49</sup> (Figure S3F); the EZH2 homolog and putative H3K27 trimethyltransferase *mes-2*<sup>57</sup> (Figure S3G); and the putative H3K27me3 demethylase *jmjd-3.2*<sup>58</sup> (Figure 3G). We found that *hrde-1* is also required for the heritable reduction of lipids (Figure S3I). Together, these findings point to small RNA and repressive histone modifications (Figure 3H) being necessary for establishing and transmitting the non-genetic hypoxia response to naive descendants.

### Hypoxia induces a heritable dysregulation of 22G-RNAs

Because we observed that the argonaute *hrde-1* is transgenerationally elevated in response to hypoxia and is necessary for the transgenerational hypoxia phenotype, we next examined whether small RNAs themselves are sufficient to recapitulate the hypoxic phenotype. We exposed WT worms to normoxia or hypoxia, extracted the small (<200 nt) and large RNAs (>200 nt) from the exposed worms, and then soaked naive worms in these extracted RNAs and performed egg-laying assays (Figure 4A). Although soaking the naive worms in the large RNAs extracted from hypoxia-treated worms had no effect on fertility, soaking the naive worms in the small RNAs extracted from hypoxia-treated worms was sufficient to reduce fertility (Figure 4B), raising the possibility that small RNAs are transmitted from hypoxia-exposed parents to their offspring to regulate the heritable fertility defect. Because *hrde-1* was necessary for the hypoxia-induced heritable fertility defect (Figure 3F), and feeding extracted small RNAs to naive worms was sufficient to recapitulate the reduced fertility, we next examined whether *hrde-1* was required for the small RNA-induced fertility reduction and the heritable dysregulation of gene expression in response to hypoxia. *Hrde-1* mutant worms did not display reduced fertility in response to feeding small RNA (sRNAs) extracted from hypoxia-exposed WT worms (Figure S4A), suggesting *hrde-1* is required for the small RNA-induced fertility reduction. Although *hrde-1* was required for the majority of hypoxia-regulated gene expression changes, a subset (475/6,814) of genes displayed a similar upregulation (red box: 60 genes) and downregulation (blue box: 415 genes) in the P0 generation of *hrde-1* mutant worms as in WT worms in response to hypoxia (Figure 4C). However, these dysregulated genes failed to be transmitted to the naive F1 *hrde-1* descendants because they were in WT worms (Figure 4C). This finding points to this subset of genes being important for the fertility phenotype and suggests that *hrde-1* is required for the transmission of the dysregulation of heritable gene expression, in addition to the transmission of the heritable fertility phenotype, in response to hypoxia.

P granules are non-membrane-bound RNA and protein condensates located adjacent to the nuclei in the germline of *C. elegans*.<sup>59</sup> These granules are postulated to regulate germ cell differentiation by playing a role in mRNA surveillance and are also postulated to potentially

sequester and transmit RNAs across generations to maintain the memory of germline gene expression.<sup>59–62</sup> We therefore examined whether transcripts reported to be contained within the P granules<sup>63</sup> were present in the set of heritable dysregulated genes in response to hypoxia. We found that ~30% of the P granule transcripts (198/660 transcripts) were present in the hypoxia-heritable upregulated genes, whereas a small minority (~1.7%, 11/660 transcripts) was present in the hypoxia-heritable downregulated genes (Figure S4B). To investigate whether the P granules themselves were dysregulated in response to hypoxia, we dissected germlines from normoxia- and hypoxia-treated worms and their normoxia-reared descendants and visualized P granules using a *pgl-1::GFP* transgenic strain.<sup>43</sup> We found that, as has been previously reported,<sup>64</sup> the P granules dissociated from the nuclei at the diplotene and diakinesis stages of meiosis and diffuse into the cytoplasm in unfertilized oocyte under normoxia conditions. Surprisingly, the P granules remained tightly bound to the nuclei through the diplotene and diakinesis stages under hypoxia conditions (Figure S4C; ~85% retention in hypoxia versus ~15% in normoxia). Although this prolonged P granule retention decreased across generations, there was an increased P granule retention in the F1 (~50%) and F2 (38%) generations before returning to basal levels in the F3 generation (Figure S4C). In addition to increased temporal retention of P granules, there was also a quantifiable increase in the number of P granules associated with the nuclei of oocytes (Figure S4C; P0:  $p < 0.001$ , F1:  $p < 0.05$ , F2:  $^{ns}p = 0.14$ , and F3:  $^{ns}p = 0.33$ , where  $^{ns}$  represents not significant). Together these results indicate that P granules are retained adjacent to nuclei in the meiotic germline for the same number of generations that there are aberrant gene expressions and a fertility reduction in response to hypoxia, raising the possibility that the extended P granule retention could facilitate the transmission of specific RNAs to descendant generations in response to hypoxia.

Because *hrde-1* is required for the transgenerational fertility decrease and gene expression dysregulation in response to hypoxia, and because the extended P granule retention tracked with the transgenerational fertility reduction, we decided to examine how aberrant small RNAs become dysregulated in response to hypoxia. We performed small RNA-seq in WT and *hrde-1* mutant worms in the P0, F1, F2, and F3 generations after P0 exposure to hypoxia. We found that our small RNA-seq in the P0 *hrde-1* mutants under normoxia conditions correlated well with published data (Figure S4D).<sup>48</sup> As has been previously shown,<sup>48</sup> in response to deletion of *hrde-1*, there is global aberrant small RNA expression (Figure 4D). Because small RNAs of hypoxiatreated worms were sufficient to induce a fertility defect, we were interested as to what categories of genes were targeted by the dysregulated small RNAs. We observed a coordinated transgenerational dysregulation of both microRNA and microRNA targets in response to parental hypoxia. To examine broadly what processes heritably misregulated microRNA target genes, we performed a Gene Ontology (GO) analysis of hypoxia-induced microRNA targets. These heritably dysregulated hypoxia microRNA targets displayed enrichment for endocytosis, cellular respiration, fatty acid oxidation, and vesicle-mediated transport, raising the possibility that the microRNAs displaying heritable changes and their targets are potentially directly regulating metabolic hypoxia-sensitive pathways and lipid synthesis (Figures S4E and S4F). Examples of transgenerational dysregulation of both microRNA and microRNA targets in response to parental hypoxia include *mir-253-3p* and *mir-39-3p* and their putative targets

*F57G12.1*<sup>65</sup> and *lin-41*<sup>66</sup> (Figures S4G and S4H). When examining predicted targeting of *mir-237*, *mir-253*, and the siRNAs that become intergenerationally and transgenerationally dysregulated, we found that the majority of the targets of these small RNAs are downregulated transgenerationally in response to parental hypoxia treatment (Figure S5I). We further found that two of the targets of intergenerationally or transgenerationally misregulated microRNAs, *mir-253-3p* and *mir-39-3p*, were necessary for the initial fertility response to hypoxia, as was the case for *F57G12.1* (Figure S3D), or for the transmission of the fertility defect to the subsequent generations, as was the case for *lin-41* (Figure S3H). These results suggest that not only the misregulated microRNAs but also their downstream targets might represent a network of responses to hypoxia that facilitate an adaptive response in both the exposed generation and the naive normoxia-reared descendants. Together, these data suggest that heritable dysregulation of specific small RNAs can induce heritable dysregulation of specific target genes.

We next focused our examination on small RNAs, which were heritably dysregulated in WT worms in response to hypoxia and showed similar dysregulation in the P0 generation of *hrde-1* mutant worms. We identified a small subset of RNAs that have a strong propensity for a 5' guanosine residue and a length of 22 nt (22G-RNAs)<sup>67</sup> that were heritably upregulated (red box: 86 22G-RNAs), in addition to another subset of 22G-RNAs that were heritably downregulated (blue box: 148 22G-RNAs), in response to parental hypoxia exposure (Figure 4D). A portion of the hypoxia-induced heritable dysregulated 22G-RNAs in WT worms was similarly dysregulated in *hrde-1* mutant worms in the parental P0 generation (17/86 upregulated and 80/148 downregulated;  $p < 0.05$ ) but failed to be transgenerationally dysregulated in *hrde-1* descendants (Figure 4D). 22G-RNAs will silence or activate genes that they target when bound to different argonautes.<sup>24</sup> Binding to HRDE-1 facilitates transcriptional silencing,<sup>19</sup> whereas binding to the chromosome segregation and RNAi-deficient (CSR-1) argonaute protein promotes nascent mRNA transcription and activates gene expression.<sup>21</sup> A comparison of hypoxia transgenerationally dysregulated genes with those previously shown to be bound by HRDE-1<sup>19</sup> and CSR-1<sup>20</sup> revealed that hypoxia transgenerationally induced genes were enriched for CSR-1-bound small RNA targets (Figure 4E; 526/1,068 hypoxia-induced heritably upregulated genes were CSR-1 targets and 59/1,068 heritably upregulated genes were HRDE-1 targets;  $p = 0$  by hypergeometric probability). Conversely, hypoxia transgenerationally downregulated genes showed a preference for HRDE-1-bound small RNA targets (Figure 4F; 129/1,326 hypoxia heritably downregulated genes were HRDE-1 targets, and 66/1,326 heritably downregulated genes were CSR-1 targets;  $p = 6E^{-4}$  by hypergeometric probability). All 22G-RNAs triggered by hypoxia that were previously shown to be bound to either worm-specific argonautes (WAGOs) or CSR-1,<sup>20</sup> as well as their target mRNAs, showed diminished changes in response to hypoxia in *hrde-1* mutant worms (Figure 4G). Most 22G-RNAs were upregulated, in a *hrde-1*-dependent manner, in response to hypoxia in the P0 generation, and were reset in naive normoxia-reared descendants (Figure 4H). However, some 22G-RNAs were heritably upregulated, such as the endogenous siRNA *F44E5.4/5* (Figure 4I). To validate the heritable increase of endogenous siRNA *F44E5.4/5* by an alternative method, we performed northern blots using probes targeting the 22G-RNA region. We found a modest but statistically significant increase in *F44E5.4/5* 22G-RNAs in both the P0 and



F1 generations of hypoxia-treated parents or worms fed with small RNAs extracted from hypoxia-treated worms (Figure S4J). Interestingly, although there is a heritable increase in endogenous siRNA *F44E5.4/5*, this is coupled with a heritable decrease in *F44E5.4/5* transcript in response to hypoxia (Figure 4I). *F44E5.4/5* is an *hsp-70*-like heat shock protein that generally functions as a protein chaperone. Interestingly, *F44E5.4/5* has been shown to be intergenerationally downregulated in response to heat shock,<sup>68</sup> suggesting that this heat shock protein might be particularly susceptible to being intergenerationally dysregulated. Taken together, we found an HRDE-1-dependent dysregulation of endogenous siRNAs in response to hypoxia, raising the possibility that those endogenous siRNAs may play a role in transmitting the memory of hypoxia from parents to their progeny.

### ***F44E5.4/5* siRNA is sufficient to induce a heritable decrease in fertility and is directly transmitted from parents to their progeny**

To determine whether we could identify specific small RNAs that were sufficient to induce fertility defects, we pared down an initial list of small RNAs that were heritably upregulated (including 6 microRNAs, 11 Piwi-interacting RNA (piRNAs), 1 small nucleolar RNA [snoRNA], and 9 22G-RNAs) based on the magnitude and/or downregulation of known target genes to 9 small RNAs (Figure 5A), to examine in more detail which were intergenerationally or transgenerationally misregulated in response to parental hypoxia treatment, including a snoRNA, *Y71D11A.7*; three endogenous siRNAs that target *T05C3.6*, *HSP-16.2*, and *F44E5.4/5*; and five microRNAs, *mir-253*, *mir-237*, *mir-1829*, *mir-4936*, and *mir-58.1* (Figure 5A). We also found that *mir-39-3* was transgenerationally upregulated in response to parental hypoxia treatment. We found that exposing normoxia-reared worms to *in-vitro*-transcribed duplexes spanning the *mir-237* region or double-stranded *F44E5.4/5* siRNAs alone was sufficient to recapitulate the fertility defects (Figure 5B). *F44E5.4/5* mRNA was reduced ~5-fold after soaking the worms in *F44E5.4/5* dsRNA (Figure S5A). The fertility defects after soaking worms in *F44E5.4/5* siRNAs, but not *mir-237*, were observed in naive F1 descendants (Figure 5C), suggesting that this siRNA is sufficient to induce an intergenerational fertility defect. Genetic knockout of *mir-237* (Figure 5D) or microinjection of an antagomir of *mir-237* (Figure 5E) revealed that *mir-237* is necessary for the hypoxia-induced fertility defect in the parental P0 generation (Figures 5D and 5E). Together, these results suggest the argonaute HRDE-1 and specific small RNAs are intergenerationally and transgenerationally misregulated in response to parental hypoxia exposure and are necessary and sufficient to regulate a heritable fertility defect in response to hypoxia exposure.

To determine whether *F44E5.4/5* siRNAs themselves were being transmitted from parents to their progeny, we *in-vitro*-transcribed *F44E5.4/5* siRNAs as before but used uridine triphosphate (UTP) that had been modified to incorporate the Cy3 fluorescent dye, administered these labeled exogenous siRNAs to naive worms, and looked for fluorescence in the F1 generation. Moreover, we performed enzymatic labeling of DNA with Cy3-dUTP through PCR and microinjected the labeled DNA or Cy3-UTP alone into P0 adults as controls. We first validated that the Cy3-labeled *F44E5.4/5* siRNAs were as efficient as the nonfluorescently labeled siRNAs at reducing fertility (Figure 5F), suggesting that the addition of the fluorescent label does not inhibit the function of *F44E5.4/5* siRNAs.

Excitingly, after injecting Cy3-labeled *F44E5.4/5* dsRNA (*F44E5.4/5::Cy3*) into young adult worms,<sup>70</sup> we could detect fluorescent signal in both P0 adults and F1 embryos (Figure 5G). Neither Cy3-UTP fluorescent dye itself nor *F44E5.4/5* dsDNA amplified incorporating Cy3 label was transmitted to F1 embryos, suggesting that this specific RNA has the capacity to be taken up by new F1 embryos when upregulated in the mother (Figure 5G). To understand whether the dsRNA was first taken up by the germline or directly transported into the existing oocytes, we microinjected the Cy3-labeled dsRNA *F44E5.4/5* into *hrde-1::GFP* transgenic worms. Because HRDE-1 is a germline argonaute localized to the nucleus,<sup>19</sup> this allowed us to visualize where *F44E5.4/5* entered the cells. We found that the dsRNA accumulated as puncta within oocytes and had the highest accumulation at the oocyte, which was proximal to the spermatheca (–1 oocyte) (Figure S5B). Furthermore, by soaking L4 worms in dsRNA *F44E5.4/5::Cy3*, we could detect labeled *F44E5.4/5* dsRNA in the F1 generation (Figure 5H). *F44E5.4/5::Cy3* dsRNA was not directly absorbed by embryos outside of their mothers (Figure S5C), suggesting that these labeled dsRNAs are transmitted across generations. Interestingly, the transmitted RNAs were polarized to the anterior side of early embryos, as assessed by localization of *F44E5.4/5::Cy3* dsRNA relative to asymmetrically enriched proteins, including the RNA-binding protein MEX-3 (Figure 5H), the intrinsically disordered RNA-binding protein MEG-3 (Figure S5D), and the guanyl-specific ribonuclease PGL-1 (Figures S5E and S5F), which are enriched in the posterior half of embryos,<sup>71–73</sup> and the Polo-like kinase protein, PLK-1, which is enriched in the anterior side<sup>74</sup> (Figure S5G). Because fluorescent signal was not detected after soaking eggs in dsRNA *F44E5.4/5::Cy3* solution (Figure S5C), exogenous siRNA *F44E5.4/5::Cy3* is presumably actively transmitted from parents to progeny rather than passively taken up through diffusion into the embryos. After *F44E5.4/5::Cy3* dsRNA microinjection into P0 adult, the fluorescent signal persisted in localized puncta in the F1 worms through the L1, L3, L4, and adult developmental stages (Figure S5H). Together, these data suggest that *F44E5.4/5* siRNA is intergenerationally upregulated in response to parental hypoxia, is transmitted across generations, and is sufficient to cause a heritable decrease in fertility.

## DISCUSSION

Here we showed that hypoxia causes an intergenerational decrease of lipids and a transgenerational reduction of fertility, which requires putative regulators of the repressive histone modifications H3K9me and H3K27me3 (*set-25*, *mes-2*, and *jmjd-3.2*), as well as the small RNA argonaute (*hrde-1*) (Figures 1, 3, S3, and S5I). We observed an intergenerational and transgenerational dysregulation of specific histone modifications, mRNAs, and small RNAs on parental hypoxia treatment (Figures 2, 4C, 4D, 5, S2, and S4). Remarkably, small RNAs (<200 nt) extracted from hypoxia-treated worms, as well as *mir-237* and siRNA *F44E5.4/5*, which were intergenerationally and transgenerationally upregulated in response to hypoxia, were sufficient to induce fertility defects in naive worms (Figures 5A, 5B, and 5F). Moreover, we found that dsRNA directed against *F44E5.4/5* was sufficient to induce an intergenerational fertility defect (Figure 5C), and we were able to directly track a Cy3-labeled *F44E5.4/5* dsRNA as being transmitted from P0 adult worms to F1 embryos in a polarized fashion (Figures 5G, 5H, and S5D–S5G). Together these data suggest that

*F44E5.4/5* siRNA is intergenerationally upregulated in response to parental hypoxia, is transmitted across generations, and is sufficient to cause a heritable decrease in fertility.

Biological processes work as a coherent system involving multifaceted components. It is clear that the transgenerational response to hypoxia involves both the chromatin-modifying machinery and small RNAs. It will be interesting in future studies to examine how hypoxia elicits the specific changes in histone methylation marks and small RNA production. Are the changes that occur in histone methylation due to misregulation of the SAM synthesis enzymes alone or also through altered function of specific histone demethylases that could require oxygen as a co-factor?<sup>75</sup> Work across several model organisms has demonstrated that small RNAs and chromatin modifications function together to reinforce an epigenetic silenced state.<sup>76</sup> Interestingly, we observed an intergenerational misregulation of lipids in response to hypoxia. Because lipids are transferred from the gut to embryos,<sup>75</sup> it will be exciting, in future experiments, to examine whether these misregulated lipids are necessary for sensing and conveying reduced oxygen availability to naive descendants. Could the altered lipid content itself be transmitted to naive descendants? It will also be important to integrate how lipid dysregulation can interact directly or indirectly with the chromatin-modifying enzymes and small RNA machinery. Additionally, previous work has shown that lipid droplets formed by neutral lipids are required for meiosis progression during yeast sporulation,<sup>77</sup> raising the possibility that the misregulation of lipids could itself be the cause of the decreased brood size in *C. elegans*. It will be important to decipher which lipids are intergenerationally misregulated and whether these specific lipids are altering the production of progeny in the P0 and F1 generation parents.

Additionally, it remains to be seen how specific small RNAs that are transmitted from parents to their descendants in response to hypoxia or other transgenerational epigenetic inheritance paradigms are selected among all the small RNAs that *C. elegans* generate. What special characteristic allows dsRNA directed against *F44E5.4/5* to be transmitted to the next generation, and does this contribute to this RNA's subcellular localization? We feel that by examining what characteristics are unique among the dysregulated small RNAs and lipids, future experiments will be able to provide answers to these important next-step questions.

Together, we dissected the critical molecular components of transgenerational epigenetic inheritance in response to hypoxia in *C. elegans*. We identified that parents utilized small RNAs to alert the future offspring of the hypoxic stress signals that they experienced to potentially prepare for lowered oxygen availability.

### Limitations of the study

The mechanisms of how *F44E5.4/5* causes direct fertility reduction and whether the endogenous siRNA recruits histone modifications marks to work together to silence gene expressions remain unclear. Because these experiments are transgenerational, it is impossible to extract different generations at the exact same time to directly compare samples across generations for bulk RNA-seq and western blotting experiments. To get around this, by necessity we froze down samples at the same developmental stage and performed the extractions and downstream analyses at the same time. This means that only pairwise comparisons of the exact same generations can be performed, and there are some

gene expression differences in normoxia controls across generations. The RNA and proteins collected reflect the average of gene and protein expressions, and therefore each generation may vary slightly. In this manuscript, we labeled and attempted to track siRNA transmission from parents to their children. Labeling, by its very nature, alters the system; however, this is the only way to visualize what is actually being inherited. We found that the labeled dsRNA was able to recapitulate the fertility defect, suggesting that the label is not altering the system too dramatically.

## STAR★METHODS

### RESOURCE AVAILABILITY

**Lead contact**—Further information and requests for resources and reagents should be directed to the lead contact, Eric Greer (Eric.Greer@childrens.harvard.edu).

**Materials availability**—The study did not generate new unique reagents and materials.

#### Data and code availability

- All the genomic sequencing datasets are deposited at the Gene Expression Omnibus GEO database and are publicly available as of the date of publication. Accession numbers are listed in the key resources table. Original unprocessed data is available via Mendeley Data at<sup>1</sup> <https://data.mendeley.com/datasets/phhyh57zsc/draft?a=b782b018-4198-4f0f-a338-311c22c0387a>
- This paper does not report original code.
- Any additional information required to reanalyze the data reported in this paper is available from the lead contact upon request.

### EXPERIMENTAL MODEL AND SUBJECT DETAILS

**C. elegans strains**—The N2 Bristol strain was used as the WT background. The following mutations were used in this study: *hrde-1(tm1200)*, *jmjd-3.1(gk384)*, *jmjd-3.1(gk387)*, *jmjd-3.2(tm3121)*, *meg-3(tm4259)*, *mes-2(bn11)* *unc-4(e120)/mnC1 [dpy-10(e128) unc-52(e444)]*, *met-2(ok2307)*, *mir-237(tm2238)*, *nrde-2(gg95)*, *sago-2(tm894)*, *set-17(n5017)/set-30(gk315)*, *set-25(n5021)*, *set-32(ok1457)*, *sid-1(qt9)*, *wdr5.1(ok1417)*, *mir-237(tm2238)*.<sup>78</sup> *Transgenes: meg-3(ax3054[meg-3::meGFP])*, *mex-3(tn1753 [gfp::3xflag::mex-3])*, *pgl-1(ax3122[pgl-1::gfp])*, *plk-1(lt18[plk-1::sGFP)::loxP]*, *glh-1(sam24[glh-1::gfp::3xFLAG])*; *itIs37[pie1p::mCherry::H2B::pie-1 3'UTR, unc-119(+)]IV*.<sup>79</sup> Worms were grown on dam-dcm-(NEB C2925) or OP50 bacteria in all experiments on standard nematode growth medium (NGM) plates.<sup>91</sup>

### METHOD DETAILS

**Antibodies**—Antibodies used for western blots were: rabbit anti-H3 (Abcam Ab1791), rabbit anti-H3K27me3 (Millipore-Sigma 07-449), rabbit anti-H3K23me3 (Active Motif 61,500), rabbit anti-H3K4me3 (Abcam Ab8580), mouse anti-H3K9me2 (Abcam Ab122),

rabbit anti-H3K9me3 (Abcam Ab8898), and rabbit anti-H3K4me1 (Abcam Ab8895). These antibodies have demonstrated specificity in eukaryotes.

**Experimental set-up**—The worms were kept at 20°C with sufficient food supply for at least 3 generations before the hypoxic exposure experiments. L4 stage worms were exposed at 0.1% oxygen level in a hypoxic chamber (Eppendorf Galaxy 48R incubator) for 16 h at 20°C, then they were returned to ambient oxygen level (~20%). Staggered normoxia reared worms were grown such that when the hypoxia treated worms recovered from the hypoxia treatment, which halted developmental progression, the control worms were at the same developmental stage.

**Fertility assay**—Ten L4 worms were placed on OP50–1 bacteria seeded normal growth media (NGM) plates<sup>91</sup> in triplicate (thirty worms per genotype) and grown at 20°C. The worms were switched to new plates every day. The numbers of hatched worms were counted. Repetition experiments were blinded and counted by a different researcher. Each mutant strain was examined in 3–11 independent triplicate experiments. Paired t-tests (two-sided) and Fisher's combined probability test were performed to compare brood sizes between each condition in every generation.

**Oil red O staining**—L4 worms in normoxic and hypoxic conditions were grown on NGM plates for a day and were stained at the gravid young adult stage. The worms were washed with PBST (0.137M NaCl, 2.7mM KCl, 10mM Na<sub>2</sub>HPO<sub>4</sub>, KH<sub>2</sub>PO<sub>4</sub> 1.8mM, 0.1% Tween 20) three times, the supernatant was removed and the worm pellet was examined. 600 µL of 40% isopropanol was added to each tube of concentrated washed worms and the worms were rocked for 3 min at room temperature. Worms were spun at 560 × g for 1 min, and all but 100 µL of supernatant was removed. 600 µLs of Oil red O working solution was diluted from original Oil Red O solution (Sigma O1391) to 60% with water and filtered through a 0.2 µm filter, and was added to each tube. Worms were rocked for 2 h at room temperature. Tubes were centrifuged at 560 × g for 1 min, and the supernatant was removed. Pellets were resuspended in 600 µL of PBST and rotated at room temperature for 30 min. The supernatant was removed, and 5 µL of worms was placed on slides and covered by a coverslip. The slides were imaged on a Zeiss Discovery V8 microscope, and the images were quantified in ImageJ (1.0).

**Lifespan assay**—Worm lifespan assays were performed at 20°C, without 5-fluoro-2'-deoxyuridine (FUdR). For each lifespan assay, ~90 worms per condition were used in three plates to begin the experiment (30 worms per plate). Worms that underwent matricide, exhibited a ruptured vulva, or crawled off the plates were censored. Statistical analyses of lifespan were performed on Kaplan-Meier survival curves in StatView 5.0.01 by log rank (Mantel-Cox) tests. The values from the Kaplan-Meier curves are included in the Table S1.

**Germ cell fixation for microscopy**—Young adults 24 h after the L4 stage were anesthetized with 15 µL of azide mix (25 mM HEPES pH 7.4, 0.118 M NaCl, 48 mM KCl, 2 mM EDTA, 0.5 mM EGTA, 0.1% Tween 20, 16.7 mM NaAzide), and 15 to 20 worms were dissected on azide mix drops. The tail or head was cut with a needle to let the entire gonad to come out. The worms were fixed with 15 µL of 2% formaldehyde for 5

min, and attached to superfrost plus slides (+), and immediately placed on a frozen block. The cover slips were scraped with a razor blade and the slide were dipped in ice-cold 97% methanol for 1 min. The slides were then dried for 1 min, washed 2 times with PBST, and mounted in Vectashield mounting medium (H-1200-10) with DAPI.

**Western blots**—Worms were lysed with RIPA buffer and quantified by Bradford assay (Biorad 5000006). Five to 10  $\mu\text{g}$  of proteins were loaded for gel electrophoresis and transferred to nitrocellulose membrane (Biorad 1620097) with 100 volts for 1.5 hours. The membranes were incubated in 5% milk for 1 hour at room temperature and incubated with primary antibodies (1:500 dilution for anti-H3K9me2, anti-H3K9me3, and anti-H3K27me3; 1:1000 dilution for anti-H3K4me1, anti-H3K4me3, and anti-H3K23me3; 1:3000 dilution for anti-H3). After washing with TBST 3 times for 10 minutes each, the membranes were incubated with secondary antibody (Millipore Rabbit IgG, Millipore Mouse IgG, 1:1000–1:3000 dilution). The blots were incubated with chemiluminescent HRP substrate (Millipore WBKLS0500) and imaged in a ChemiDoc Touch Imaging System (Biorad).

**Small RNA extraction and administration**—To isolate large RNAs (>200 nt) and small RNAs (<200 nt) from worms, mirVana miRNA Isolation kit (life technologies) was used as per kit protocol. Briefly, 100  $\mu\text{L}$  of Lysis/Binding Buffer was added to the frozen samples on ice and homogenized with a pellet pestle motor (Kontes). 1/10 volumes of miRNA homogenate additive were added, and an equal volume of acid-phenol:chloroform was added, samples were then vortexed and centrifuged for 5 min at  $10,000 \times g$ . For isolation of large RNAs (>200 nt), 1/3<sup>rd</sup> volume of 100% ethanol was added to the aqueous phase recovered from organic extraction, and a filter cartridge was used to separate large RNAs and small RNAs by centrifugation, and the large RNAs were collected on the column filter. To isolate small RNAs (<200 nt), 2/3<sup>rd</sup> volume of 100% ethanol was added to the flow-through and collected in a different filter cartridge. The columns were washed with 700  $\mu\text{L}$  of miRNA wash solution 1, and washed twice with wash solution 2, and eluted in nuclease-free water. The large RNAs and small RNAs extracted from normoxic and hypoxic worms were administered to naive worms at L4 stage at the concentration of 0.2  $\mu\text{g}/\mu\text{L}$  by soaking the worms in the RNA solution for 16 h at 18°C.

**In vitro transcription of dsRNA and administration of small RNAs**—PCR templates containing T7 promoters on both ends of double strand DNA for each candidate were *in vitro* transcribed with Hi-Scribe T7 quick high yield RNA synthesis kit (NEB E2050) as per the companies protocol. For standard dsRNA synthesis, 500 ng to 1  $\mu\text{g}$  of DNA was used as the starting material, and mixed with 10  $\mu\text{L}$  NTP buffer mix and 2  $\mu\text{L}$  T7 RNA polymerase mix in a 30  $\mu\text{L}$  reaction, and incubated at 37°C overnight. For the dsRNA synthesis with modified nucleotides (Cyanine3-UTP), 5 mM Cy3-UTP (enzolifesciences ENZ-42505) was added to 5  $\mu\text{L}$  of dNTPs (5 mM of each dNTP) and with 2  $\mu\text{L}$  T7 RNA polymerase mix in a 20  $\mu\text{L}$  reaction and incubated at 37°C overnight. To remove the template DNA, 2  $\mu\text{L}$  of DNase was added to the reaction and incubated for 15 min at 37°C. The newly synthesized dsRNA was purified using the Monarch RNA cleanup kit (NEB T2040). To label the dsDNA with Cyanine-3, a Cy3 PCR labeling kit (Jena Bioscience PP-301S-CY3) was used. The labeled dsRNAs, dsDNA,

and Cyanine-3 UTP alone were administered through either soaking method as described above or by microinjection using the method described in<sup>87</sup> and<sup>92</sup> For microRNA antagomir administration, 50  $\mu$ M of cel-miR-237-5p antagomir (mirVana miRNA inhibitor) with the mature sequence: UCCCUGAGAAUUCUCGAACAGCU was co-injected with *in vitro* transcribed unc-22 dsRNA (1  $\mu$ g/ $\mu$ L). Successful delivery of antagomirs was assessed by observation of an uncoordinated phenotype.

**RNAseq**—Two 60  $\times$  15 mm plates of worms where the parental generation was treated with normoxia or hypoxia were synchronized at L4/post L4 stage for sample collection of P0, F1, F2, and F3 generations for WT and *hrde-1* mutant worms. Whole worms were lysed using a tissue homogenizer (Kontes) and total RNA was extracted using mirVana miRNA Isolation kit (life technologies). Messenger RNAs were enriched using NEXTFLEX Poly A Beads 2.0. Two biological replicates were produced for each condition. In total, 32 samples were prepared for RNA-seq libraries with 500 ng mRNA as starting materials using NEXTflex Illumina qRNA-Seq Library Prep Kit (Bio Scientific) as per the manufacturers protocol. In short, mRNA was fragmented in a cationic buffer and underwent first and second strand synthesis, adenylation, molecular index adapter ligation and 11 cycles of PCR amplification. The amplified products were cleaned by Agencourt AmPure XP Magnetic Beads (Beckman Coulter) and RNA quality was validated by Agilent 2200 TapeStation D1000. The optimal cluster density was determined by KAPA library quantification kit before pooling the samples into a pooled library (5 nM) and sequencing using a Nextseq 500 platform.

The fastq files were filtered with a Q score of 30 or above and were trimmed for the sequencing adaptors using CutAdapt (version 2.5). The sequencing reads were aligned to the *C. elegans* genome (WS235) by bowtie2. Transcript and gene expression matrices were built with rsem-generate-data-matrix function in RSEM pipeline.<sup>80</sup> For calling the significant differentially expressed genes (DEGs), the false discovery rate (FDR) after multiple testing correction was set as 0.05 and analyzed in edgeR.<sup>81</sup>

**Small RNAseq**—The small RNAs of hypoxia and normoxia reared P0, F1, F2, and F3 worms from WT and *hrde-1* mutants were extracted using the mirVana miRNA Isolation kit (life technologies) described above from the same worm samples used to generate RNAseq cohorts. 500 ngs of total RNA was treated with RNA 5' pyrophosphohydrolase (RppH) (NEB #M0356) at 37°C for 30 min, to ensure 5' monophosphate-independent capture of small RNAs. 500 mM EDTA was added to stop the reaction which was then cleaned up in RNA Clean & Concentrator-5 (Zymo 11-352) and eluted in nuclease free water. Around 100–300 ng of total RNAs including small RNAs (larger than 17 nt) were used as the starting material for library preparation using Nextflex Small RNA-seq Kit v3 (NOVA-5132-06) as per the manufacturers protocol. The RNAs were denatured at 70°C and ligated at the 3' position as well as the 5' position with 4N adaptors. The ligated RNAs were reverse transcribed and amplified for 12–17 cycles in PCR reactions. The libraries were cleaned up with Nextflex beads, and the quality of the RNAs was examined by an Agilent 2200 TapeStation D1000 before single end sequencing on an Illumina NextSeq 500 machine with High output kit (1–75 cycle).

The illumine fastq files were assessed for quality with FastQC. The 3' adaptors (TGGAATTCTCGGGTGCCAAGG) were removed and the 4 random bases at both 5' AND-3' ends were trimmed with cutadapt (version 2.5). The clipped reads were mapped to the *C. elegans* genome WS277 assembly with shortstack<sup>82</sup> and allowing 1 mismatch. Count tables were generated with featurecount<sup>83</sup> and the differential analysis was performed in edgeR<sup>81</sup> with web-based tool DeApp.<sup>84</sup>

**Quantitative real-time PCR (qRT-PCR)**—Total RNA was extracted from *C. elegans* using Invitrogen PureLink RNA Mini Kit (Invitrogen, 12183018A). First strand cDNA synthesis was conducted using SuperScript III First-Strand Synthesis (Invitrogen, 18,080,051). qRT-PCR of cDNA was performed using iTaq Universal SYBR Green Supermix (Bio-Rad, 172–5122) on a CFX96 Real-Time System (Bio-Rad). The PCR assay contained 1:4 diluted reverse transcription products, 1X master mix, and 200 nM of each primer, and was performed with 5-min initial denaturation at 95°C followed by 40 cycles of 95°C for 5 s and 60°C for 45 s. The actin gene (*act-1*) of was used for internal normalization for each gene. The comparative Ct method (Ct) was used to calculate gene expression.

**Northern blot**—The small RNAs worms from were extracted using the mirVana miRNA Isolation kit (life technologies) described above. Probes modified with biotin on the 5' or 3' terminus were synthesized and purified through HPLC by the GenScript Company and the probes were deisgned to be complementary to target siRNAs. The siRNA probe sequences are listed in STAR method. The small RNAs were mixed with loading buffer (5 mM EDTA, 0.1% bromophenol blue, 0.1% xylene cyanol, and 95% formamide), denatured at 70°C for 5 min before loading into The Novex TBE-Urea gel (15%) (Invitrogen). The gel was run at 40 mA for 45 min, and transferred to N + positively charged nylon membranes (GE healthcare, USA) using XCell Surelock Blot module (Thermo Fisher) at 10 V for 3 h. Then, the membranes were crosslinked at 1200 μjoules for 20 min. The membranes were prehybridized for 3 h at 40°C in the prehybridization buffer ((7% SDS, 200 mM Na2HPO4 (pH 7.0), 5 μg/mL salmon sperm DNA (SSDNA)), and further hybridized with the probes in the NorthernMax hybridization buffer (Thermo Fisher) overnight at 40°C. The biotin-labeld probes were detected using a Chemiluminescent Nucleic Acid Detection Module Kit (Thermo Scientific, USA) and imaged in a ChemiDoc Touch Imaging System (Biorad).

**Visualization and statistics**—The genome browser snapshots were generated using IGV (2.8.2),<sup>85</sup> and all the figures were generated using adobe illustrator 2020. The Gene-set enrichment analyses were performed using Wormcat<sup>86</sup> and WebGestalt.<sup>88</sup> Heatmap was generated with iDEP v0.93beta.<sup>89</sup> The RNAseq and small RNAseq reads in F2 normoxia groups were normalized with F1 and F3 normoxia groups to account for batch effects. The microRNAs and gene targets were visualized in a miRNA-centric network visual analytics platform (miRNet).<sup>90</sup>

## QUANTIFICATION AND STATISTICAL ANALYSIS

Statistics and graphing were conducted in Prism 9. Equality of variance was checked with F test, and parametric Tuckey t test (two-sided) was used, otherwise the nonparametric



Mann Whitney t test (two-sided) was used. Fisher's exact test was performed for combining multiple independent experiments and Hypergeometric Probability test was used to test the independence of categories were each used as indicated in the figure legends. Additional statistical details including the number of replicates and numbers of animals used are indicated in the figure legends.

## Supplementary Material

Refer to Web version on PubMed Central for supplementary material.

## ACKNOWLEDGMENTS

We thank S. Strome, D. Updike, and members of the Greer lab for discussions. We thank V. Ambros for critical reading of the manuscript. We thank A. Grishok, D. Updike, F. Slack, and the Caenorhabditis Genetics Center, which is funded by NIH Office of Research Infrastructure Programs (P40 OD010440), for *C. elegans* strains. S.Y.W. was supported by Croucher Foundation and Charles King fellowships. Z.K.O. was supported by T32-HD007466. This work was supported by NIH grants (R00AG043550 and DP2AG055947 to E.L.G.).

## REFERENCES

1. Wang SY, Kim K, O'Brown ZK, Levan A, Dodson AE, Kennedy SG, Chernoff C, and Greer EL (2022). Hypoxia induces transgenerational epigenetic inheritance of small RNAs. *Mendeley Data*. 10.17632/phhyh17657zsc.17631.
2. Avery OT, Macleod CM, and McCarty M (1944). Studies on the chemical nature of the substance inducing transformation of pneumococcal types : induction of transformation by a desoxyribonucleic acid fraction isolated from pneumococcus type iii. *J. Exp. Med.* 79, 137–158. 10.1084/jem.79.2.137. [PubMed: 19871359]
3. Halfmann R, Jarosz DF, Jones SK, Chang A, Lancaster AK, and Lindquist S (2012). Prions are a common mechanism for phenotypic inheritance in wild yeasts. *Nature* 482, 363–368. 10.1038/nature10875. [PubMed: 22337056]
4. Rangunathan K, Jih G, and Moazed D (2015). Epigenetics. Epigenetic inheritance uncoupled from sequence-specific recruitment. *Science* 348, 1258699. 10.1126/science.1258699. [PubMed: 25831549]
5. Greer EL, Maures TJ, Ucar D, Hauswirth AG, Mancini E, Lim JP, Benayoun BA, Shi Y, and Brunet A (2011). Transgenerational epigenetic inheritance of longevity in *Caenorhabditis elegans*. *Nature* 479, 365–371. 10.1038/nature10572. [PubMed: 22012258]
6. Dias BG, and Ressler KJ (2014). Parental olfactory experience influences behavior and neural structure in subsequent generations. *Nat. Neurosci.* 17, 89–96. 10.1038/nn.3594. [PubMed: 24292232]
7. Brink RA (1956). A genetic change associated with the R locus in maize which is directed and potentially reversible. *Genetics* 41, 872–889. [PubMed: 17247669]
8. Padmanabhan N, Jia D, Geary-Joo C, Wu X, Ferguson-Smith AC, Fung E, Bieda MC, Snyder FF, Gravel RA, Cross JC, and Watson ED (2013). Mutation in folate metabolism causes epigenetic instability and transgenerational effects on development. *Cell* 155, 81–93. 10.1016/j.cell.2013.09.002. [PubMed: 24074862]
9. Liberman N, Wang SY, and Greer EL (2019). Transgenerational epigenetic inheritance: from phenomena to molecular mechanisms. *Curr. Opin. Neurobiol.* 59, 189–206. 10.1016/j.conb.2019.09.012. [PubMed: 31634674]
10. Greer EL, and Shi Y (2012). Histone methylation: a dynamic mark in health, disease and inheritance. *Nat. Rev. Genet.* 13, 343–357. 10.1038/nrg3173. [PubMed: 22473383]
11. Heard E, and Martienssen RA (2014). Transgenerational epigenetic inheritance: myths and mechanisms. *Cell* 157, 95–109. 10.1016/j.cell.2014.02.045. [PubMed: 24679529]

12. Moazed D (2011). Mechanisms for the inheritance of chromatin States. *Cell* 146, 510–518. 10.1016/j.cell.2011.07.013. [PubMed: 21854979]
13. Rechavi O, Minevich G, and Hobert O (2011). Transgenerational inheritance of an acquired small RNA-based antiviral response in *C. elegans*. *Cell* 147, 1248–1256. 10.1016/j.cell.2011.10.042. [PubMed: 22119442]
14. Rechavi O, Houri-Ze'evi L, Anava S, Goh WSS, Kerk SY, Hannon GJ, and Hobert O (2014). Starvation-induced transgenerational inheritance of small RNAs in *C. elegans*. *Cell* 158, 277–287. 10.1016/j.cell.2014.06.020. [PubMed: 25018105]
15. Moore RS, Kaletsky R, and Murphy CT (2019). Piwi/PRG-1 argonaute and TGF-beta mediate transgenerational learned pathogenic avoidance. *Cell* 177, 1827–1841.e12, e1812. 10.1016/j.cell.2019.05.024. [PubMed: 31178117]
16. Kaletsky R, Moore RS, Vrla GD, Parsons LR, Gitai Z, and Murphy CT (2020). *C. elegans* interprets bacterial non-coding RNAs to learn pathogenic avoidance. *Nature* 586, 445–451. 10.1038/s41586-020-2699-5. [PubMed: 32908307]
17. Posner R, Toker IA, Antonova O, Star E, Anava S, Azmon E, Hendricks M, Bracha S, Gingold H, and Rechavi O (2019). Neuronal small RNAs control behavior transgenerationally. *Cell* 177, 1814–1826.e15, e1815. 10.1016/j.cell.2019.04.029. [PubMed: 31178120]
18. Okabe E, Uno M, Kishimoto S, and Nishida E (2021). Intertissue small RNA communication mediates the acquisition and inheritance of hormesis in *Caenorhabditis elegans*. *Commun. Biol.* 4, 207. 10.1038/s42003-021-01692-3. [PubMed: 33594200]
19. Buckley BA, Burkhart KB, Gu SG, Spracklin G, Kershner A, Fritz H, Kimble J, Fire A, and Kennedy S (2012). A nuclear Argonaute promotes multigenerational epigenetic inheritance and germline immortality. *Nature* 489, 447–451. 10.1038/nature11352. [PubMed: 22810588]
20. Claycomb JM, Batista PJ, Pang KM, Gu W, Vasale JJ, van Wolfswinkel JC, Chaves DA, Shirayama M, Mitani S, Ketting RF, et al. (2009). The Argonaute CSR-1 and its 22G-RNA cofactors are required for holocentric chromosome segregation. *Cell* 139, 123–134. 10.1016/j.cell.2009.09.014. [PubMed: 19804758]
21. Seth M, Shirayama M, Gu W, Ishidate T, Conte D Jr., and Mello CC (2013). The *C. elegans* CSR-1 argonaute pathway counteracts epigenetic silencing to promote germline gene expression. *Dev. Cell* 27, 656–663. 10.1016/j.devcel.2013.11.014. [PubMed: 24360782]
22. Verdell A, Jia S, Gerber S, Sugiyama T, Gygi S, Grewal SIS, and Moazed D (2004). RNAi-mediated targeting of heterochromatin by the RITS complex. *Science* 303, 672–676. 10.1126/science.1093686. [PubMed: 14704433]
23. Mao H, Zhu C, Zong D, Weng C, Yang X, Huang H, Liu D, Feng X, and Guang S (2015). The nrde pathway mediates small-RNA-directed histone H3 lysine 27 trimethylation in *Caenorhabditis elegans*. *Curr. Biol.* 25, 2398–2403. 10.1016/j.cub.2015.07.051. [PubMed: 26365259]
24. Gushchanskaia ES, Esse R, Ma Q, Lau NC, and Grishok A (2019). Interplay between small RNA pathways shapes chromatin landscapes in *C. elegans*. *Nucleic Acids Res.* 47, 5603–5616. 10.1093/nar/gkz275. [PubMed: 31216042]
25. Lev I, Seroussi U, Gingold H, Bril R, Anava S, and Rechavi O (2017). MET-2-Dependent H3K9 methylation suppresses transgenerational small RNA inheritance. *Curr. Biol.* 27, 1138–1147. 10.1016/j.cub.2017.03.008. [PubMed: 28343968]
26. Ashe A, Sapetschnig A, Weick EM, Mitchell J, Bagijn MP, Cording AC, Doebley AL, Goldstein LD, Lehrbach NJ, Le Pen J, et al. (2012). piRNAs can trigger a multigenerational epigenetic memory in the germline of *C. elegans*. *Cell* 150, 88–99. 10.1016/j.cell.2012.06.018. [PubMed: 22738725]
27. Mette MF, Aufsatz W, van der Winden J, Matzke MA, and Matzke AJ (2000). Transcriptional silencing and promoter methylation triggered by double-stranded RNA. *EMBO J.* 19, 5194–5201. 10.1093/emboj/19.19.5194. [PubMed: 11013221]
28. Pal-Bhadra M, Leibovitch BA, Gandhi SG, Chikka MR, Rao M, Bhadra U, Birchler JA, and Elgin SCR (2004). Heterochromatic silencing and HP1 localization in *Drosophila* are dependent on the RNAi machinery. *Science* 303, 669–672. 10.1126/science.1092653. [PubMed: 14752161]

29. Kim DH, Villeneuve LM, Morris KV, and Rossi JJ (2006). Argonaute-1 directs siRNA-mediated transcriptional gene silencing in human cells. *Nat. Struct. Mol. Biol.* 13, 793–797. 10.1038/nsmbl1142. [PubMed: 16936726]
30. Kalinava N, Ni JZ, Peterman K, Chen E, and Gu SG (2017). Decoupling the downstream effects of germline nuclear RNAi reveals that H3K9me3 is dispensable for heritable RNAi and the maintenance of endogenous siRNA-mediated transcriptional silencing in *Caenorhabditis elegans*. *Epigenet. Chromatin* 10, 6. 10.1186/s13072-017-0114-8.
31. Spracklin G, Fields B, Wan G, Becker D, Wallig A, Shukla A, and Kennedy S (2017). The RNAi inheritance machinery of *Caenorhabditis elegans*. *Genetics* 206, 1403–1416. 10.1534/genetics.116.198812. [PubMed: 28533440]
32. Schwartz-Orbach L, Zhang C, Sidoli S, Amin R, Kaur D, Zhebrun A, Ni J, and Gu SG (2020). *Caenorhabditis elegans* nuclear RNAi factor SET-32 deposits the transgenerational histone modification. *Elife* 9, e54309. 10.7554/eLife.54309. [PubMed: 32804637]
33. Semenza GL (2016). The hypoxic tumor microenvironment: a driving force for breast cancer progression. *Biochim. Biophys. Acta* 1863, 382–391. 10.1016/j.bbamcr.2015.05.036. [PubMed: 26079100]
34. Fajersztajn L, and Veras MM (2017). Hypoxia: from placental development to fetal programming. *Birth Defects Res.* 109, 1377–1385. 10.1002/bdr2.1142. [PubMed: 29105382]
35. Bulterys MG, Greenland S, and Kraus JF (1990). Chronic fetal hypoxia and sudden infant death syndrome: interaction between maternal smoking and low hematocrit during pregnancy. *Pediatrics* 86, 535–540. [PubMed: 2216618]
36. Watson JA, Watson CJ, McCann A, and Baugh J (2010). Epigenetics, the epicenter of the hypoxic response. *Epigenetics* 5, 293–296. 10.4161/epi.5.4.11684. [PubMed: 20418669]
37. Chakraborty AA, Laukka T, Myllykoski M, Ringel AE, Booker MA, Tolstorukov MY, Meng YJ, Meier SR, Jennings RB, Creech AL, et al. (2019). Histone demethylase KDM6A directly senses oxygen to control chromatin and cell fate. *Science* 363, 1217–1222. 10.1126/science.aaw1026. [PubMed: 30872525]
38. Wang SY, Lau K, Lai KP, Zhang JW, Tse ACK, Li JW, Tong Y, Chan TF, Wong CKC, Chiu JMY, et al. (2016). Hypoxia causes transgenerational impairments in reproduction of fish. *Nat. Commun.* 7, 12114. 10.1038/ncomms12114. [PubMed: 27373813]
39. Lai KP, Wang SY, Li JW, Tong Y, Chan TF, Jin N, Tse A, Zhang JW, Wan MT, Tam N, et al. (2019). Hypoxia causes transgenerational impairment of ovarian development and hatching success in fish. *Environ. Sci. Technol.* 53, 3917–3928. 10.1021/acs.est.8b07250. [PubMed: 30844260]
40. Leiser SF, Fletcher M, Begun A, and Kaeberlein M (2013). Life-span extension from hypoxia in *Caenorhabditis elegans* requires both HIF-1 and DAF-16 and is antagonized by SKN-1. *J. Gerontol. A Biol. Sci. Med. Sci.* 68, 1135–1144. 10.1093/gerona/glt016. [PubMed: 23419779]
41. Heimbucher T, Hog J, Gupta P, and Murphy CT (2020). PQM-1 controls hypoxic survival via regulation of lipid metabolism. *Nat. Commun.* 11, 4627. 10.1038/s41467-020-18369-w. [PubMed: 33009389]
42. Pender CL, and Horvitz HR (2018). Hypoxia-inducible factor cell non-autonomously regulates *C. elegans* stress responses and behavior via a nuclear receptor. *Elife* 7, e36828. 10.7554/eLife.36828. [PubMed: 30010540]
43. Proescher F (1927). Oil red O pyridin, A rapid fat stain. *Stain Technol.* 2, 60–61.
44. Hendriks GJ, Gaidatzis D, Aeschmann F, and Großhans H (2014). Extensive oscillatory gene expression during *C. elegans* larval development. *Mol. Cell* 53, 380–392. 10.1016/j.molcel.2013.12.013. [PubMed: 24440504]
45. Greer EL, Beese-Sims SE, Brookes E, Spadafora R, Zhu Y, Rothbart SB, Aristizábal-Corrales D, Chen S, Badeaux AI, Jin Q, et al. (2014). A histone methylation network regulates transgenerational epigenetic memory in *C. elegans*. *Cell Rep.* 7, 113–126. 10.1016/j.celrep.2014.02.044. [PubMed: 24685137]
46. Kalinava N, Ni JZ, Gajic Z, Kim M, Ushakov H, and Gu SG (2018). *C. elegans* heterochromatin factor SET-32 plays an essential role in transgenerational establishment of nuclear RNAi-mediated

- epigenetic silencing. *Cell Rep.* 25, 2273–2284.e3, e2273. 10.1016/j.celrep.2018.10.086. [PubMed: 30463021]
47. Klosin A, Casas E, Hidalgo-Carcedo C, Vavouri T, and Lehner B (2017). Transgenerational transmission of environmental information in *C. elegans*. *Science* 356, 320–323. 10.1126/science.aah6412. [PubMed: 28428426]
  48. Ni JZ, Kalinava N, Chen E, Huang A, Trinh T, and Gu SG (2016). A transgenerational role of the germline nuclear RNAi pathway in repressing heat stress-induced transcriptional activation in *C. elegans*. *Epigenet. Chromatin* 9, 3. 10.1186/s13072-016-0052-x.
  49. Towbin BD, González-Aguilera C, Sack R, Gaidatzis D, Kalck V, Meister P, Askjaer P, and Gasser SM (2012). Step-wise methylation of histone H3K9 positions heterochromatin at the nuclear periphery. *Cell* 150, 934–947. 10.1016/j.cell.2012.06.051. [PubMed: 22939621]
  50. Cantoni GL (1952). The nature of the active methyl donor formed enzymatically from l-methionine and ADENOSINETRIPHOSPHATE1, 2. *J. Am. Chem. Soc.* 74, 2942–2943. 10.1021/ja01131a519.
  51. Batie M, Frost J, Frost M, Wilson JW, Schofield P, and Rocha S (2019). Hypoxia induces rapid changes to histone methylation and reprograms chromatin. *Science* 363, 1222–1226. 10.1126/science.aau5870. [PubMed: 30872526]
  52. Jose AM, Smith JJ, and Hunter CP (2009). Export of RNA silencing from *C. elegans* tissues does not require the RNA channel SID-1. *Proc. Natl. Acad. Sci. USA* 106, 2283–2288. 10.1073/pnas.0809760106. [PubMed: 19168628]
  53. Yigit E, Batista PJ, Bei Y, Pang KM, Chen CCG, Tolia NH, Joshua-Tor L, Mitani S, Simard MJ, and Mello CC (2006). Analysis of the *C. elegans* Argonaute family reveals that distinct Argonautes act sequentially during RNAi. *Cell* 127, 747–757. 10.1016/j.cell.2006.09.033. [PubMed: 17110334]
  54. Guang S, Bchner AF, Burkhart KB, Burton N, Pavelec DM, and Kennedy S (2010). Small regulatory RNAs inhibit RNA polymerase II during the elongation phase of transcription. *Nature* 465, 1097–1101. 10.1038/nature09095. [PubMed: 20543824]
  55. Agger K, Cloos PAC, Christensen J, Pasini D, Rose S, Rappsilber J, Issaeva I, Canaani E, Salcini AE, and Helin K (2007). UTX and JMJD3 are histone H3K27 demethylases involved in HOX gene regulation and development. *Nature* 449, 731–734, nature06145 [pii]. 10.1038/nature06145. [PubMed: 17713478]
  56. Smith J, Calidas D, Schmidt H, Lu T, Rasoloson D, and Seydoux G (2016). Spatial patterning of P granules by RNA-induced phase separation of the intrinsically-disordered protein MEG-3. *Elife* 5, 10.7554/eLife.21337.
  57. Bender LB, Cao R, Zhang Y, and Strome S (2004). The MES-2/MES-3/MES-6 complex and regulation of histone H3 methylation in *C. elegans*. *Curr. Biol.* 14, 1639–1643. 10.1016/j.cub.2004.08.062. [PubMed: 15380065]
  58. Vandamme J, Lettier G, Sidoli S, Di Schiavi E, Nørregaard Jensen O, and Salcini AE (2012). The *C. elegans* H3K27 demethylase UTX-1 is essential for normal development, independent of its enzymatic activity. *PLoS Genet.* 8, e1002647. 10.1371/journal.pgen.1002647. [PubMed: 22570628]
  59. Seydoux G (2018). The P granules of *C. elegans*: a genetic model for the study of RNA-protein condensates. *J. Mol. Biol.* 430, 4702–4710. 10.1016/j.jmb.2018.08.007. [PubMed: 30096346]
  60. Seydoux G, and Fire A (1994). Soma-germline asymmetry in the distributions of embryonic RNAs in *Caenorhabditis elegans*. *Development* 120, 2823–2834. [PubMed: 7607073]
  61. Dodson AE, and Kennedy S (2019). Germ granules coordinate RNA-based epigenetic inheritance pathways. *Dev. Cell* 50, 704–715.e4, e704. 10.1016/j.devcel.2019.07.025. [PubMed: 31402284]
  62. Wang JT, and Seydoux G (2014). P granules. *Curr. Biol.* 24, R637–R638. 10.1016/j.cub.2014.06.018. [PubMed: 25050955]
  63. Lee CYS, Putnam A, Lu T, He S, Ouyang JPT, and Seydoux G (2020). Recruitment of mRNAs to P granules by condensation with intrinsically-disordered proteins. *Elife* 9, e52896. 10.7554/eLife.52896. [PubMed: 31975687]
  64. Updike D, and Strome S (2010). P granule assembly and function in *Caenorhabditis elegans* germ cells. *J. Androl.* 31, 53–60. 10.2164/jandrol.109.008292. [PubMed: 19875490]

65. Zisoulis DG, Lovci MT, Wilbert ML, Hutt KR, Liang TY, Pasquinelli AE, and Yeo GW (2010). Comprehensive discovery of endogenous Argonaute binding sites in *Caenorhabditis elegans*. *Nat. Struct. Mol. Biol.* 17, 173–179. 10.1038/nsmb.1745. [PubMed: 20062054]
66. Lewis BP, Burge CB, and Bartel DP (2005). Conserved seed pairing, often flanked by adenosines, indicates that thousands of human genes are microRNA targets. *Cell* 120, 15–20. 10.1016/j.cell.2004.12.035. [PubMed: 15652477]
67. Gu W, Shirayama M, Conte D Jr., Vasale J, Batista PJ, Claycomb JM, Moresco JJ, Youngman EM, Keys J, Stoltz MJ, et al. (2009). Distinct argonaute-mediated 22G-RNA pathways direct genome surveillance in the *C. elegans* germline. *Mol. Cell* 36, 231–244. 10.1016/j.molcel.2009.09.020. [PubMed: 19800275]
68. Das S, Min S, and Prahlad V (2021). Gene bookmarking by the heat shock transcription factor programs the insulin-like signaling pathway. *Mol. Cell* 81, 4843–4860.e8, e4848. 10.1016/j.molcel.2021.09.022. [PubMed: 34648748]
69. Huang NN, and Hunter CP (2015). The RNA binding protein MEX-3 retains asymmetric activity in the early *Caenorhabditis elegans* embryo in the absence of asymmetric protein localization. *Gene* 554, 160–173. 10.1016/j.gene.2014.10.042. [PubMed: 25445286]
70. Marré J, Traver EC, and Jose AM (2016). Extracellular RNA is transported from one generation to the next in *Caenorhabditis elegans*. *Proc. Natl. Acad. Sci. USA* 113, 12496–12501. 10.1073/pnas.1608959113. [PubMed: 27791108]
71. Schmidt H, Putnam A, Rasoloson D, and Seydoux G (2021). Protein-based condensation mechanisms drive the assembly of RNA-rich P granules. *Elife* 10, e63698. 10.7554/eLife.63698. [PubMed: 34106046]
72. Marnik EA, and Updike DL (2019). Membraneless organelles: P granules in *Caenorhabditis elegans*. *Traffic* 20, 373–379. 10.1111/tra.12644. [PubMed: 30924287]
73. Kawasaki I, Shim YH, Kirchner J, Kaminker J, Wood WB, and Strome S (1998). PGL-1, a predicted RNA-binding component of germ granules, is essential for fertility in *C. elegans*. *Cell* 94, 635–645. [PubMed: 9741628]
74. Han B, Antkowiak KR, Fan X, Rutigliano M, Ryder SP, and Griffin EE (2018). Polo-like kinase couples cytoplasmic protein gradients in the *C. elegans* zygote. *Curr. Biol.* 28, 60–69.e8. 10.1016/j.cub.2017.11.048. [PubMed: 29276126]
75. Perez MF, and Lehner B (2019). Vitellogenins - yolk gene function and regulation in *Caenorhabditis elegans*. *Front. Physiol.* 10, 1067. 10.3389/fphys.2019.01067. [PubMed: 31551797]
76. Holoch D, and Moazed D (2015). RNA-mediated epigenetic regulation of gene expression. *Nat. Rev. Genet.* 16, 71–84. 10.1038/nrg3863. [PubMed: 25554358]
77. Hsu TH, Chen RH, Cheng YH, and Wang CW (2017). Lipid droplets are central organelles for meiosis II progression during yeast sporulation. *Mol. Biol. Cell* 28, 440–451. 10.1091/mbc.E16-06-0375. [PubMed: 27932491]
78. Metheetrairut C, Adams BD, Nallur S, Weidhaas JB, and Slack FJ (2017). *cel-mir-237* and its homologue, *hsa-miR-125b*, modulate the cellular response to ionizing radiation. *Oncogene* 36, 512–524. 10.1038/onc.2016.222. [PubMed: 27321180]
79. Marnik EA, Fuqua JH, Sharp CS, Rochester JD, Xu EL, Holbrook SE, and Updike DL (2019). Germline maintenance through the multifaceted activities of GLH/vasa in *Caenorhabditis elegans* P granules. *Genetics* 213, 923–939. 10.1534/genetics.119.302670. [PubMed: 31506335]
80. Li B, and Dewey CN (2011). RSEM: accurate transcript quantification from RNA-Seq data with or without a reference genome. *BMC Bioinf.* 12, 323. 10.1186/1471-2105-12-323.
81. Robinson MD, McCarthy DJ, and Smyth GK (2010). edgeR: a Bioconductor package for differential expression analysis of digital gene expression data. *Bioinformatics* 26, 139–140. 10.1093/bioinformatics/btp616. [PubMed: 19910308]
82. Axtell MJ (2013). ShortStack: comprehensive annotation and quantification of small RNA genes. *RNA* 19, 740–751. 10.1261/rna.035279.112. [PubMed: 23610128]
83. Liao Y, Smyth GK, and Shi W (2014). featureCounts: an efficient general purpose program for assigning sequence reads to genomic features. *Bioinformatics* 30, 923–930. 10.1093/bioinformatics/btt656. [PubMed: 24227677]

84. Li Y, and Andrade J (2017). DEApp: an interactive web interface for differential expression analysis of next generation sequence data. *Source Code Biol. Med.* 12, 2. 10.1186/s13029-017-0063-4. [PubMed: 28174599]
85. Thorvaldsdóttir H, Robinson JT, and Mesirov JP (2013). Integrative Genomics Viewer (IGV): high-performance genomics data visualization and exploration. *Brief. Bioinform.* 14, 178–192. 10.1093/bib/bbs017. [PubMed: 22517427]
86. Holdorf AD, Higgins DP, Hart AC, Boag PR, Pazour GJ, Walhout AJM, and Walker AK (2020). WormCat: an online tool for annotation and visualization of *Caenorhabditis elegans* genome-scale data. *Genetics* 214, 279–294. 10.1534/genetics.119.302919. [PubMed: 31810987]
87. Fire A (1986). Integrative transformation of *Caenorhabditis elegans*. *EMBO J.* 5, 2673–2680. [PubMed: 16453714]
88. Zhang B, Kirov S, and Snoddy J (2005). WebGestalt: an integrated system for exploring gene sets in various biological contexts. *Nucleic Acids Res.* 33, W741–W748. 10.1093/nar/gki475. [PubMed: 15980575]
89. Ge SX, Son EW, and Yao R (2018). iDEP: an integrated web application for differential expression and pathway analysis of RNA-Seq data. *BMC Bioinf.* 19, 534. 10.1186/s12859-018-2486-6.
90. Chang L, Zhou G, Soufan O, and Xia J (2020). miRNet 2.0: network-based visual analytics for miRNA functional analysis and systems biology. *Nucleic Acids Res.* 48, W244–W251. 10.1093/nar/gkaa467. [PubMed: 32484539]
91. Brenner S (1974). The genetics of *Caenorhabditis elegans*. *Genetics* 77, 71–94. [PubMed: 4366476]
92. Mello CC, Kramer JM, Stinchcomb D, and Ambros V (1991). Efficient gene transfer in *C.elegans*: extrachromosomal maintenance and integration of transforming sequences. *The EMBO Journal* 10, 3959–3970. [PubMed: 1935914]

**Highlights**

- Hypoxia causes intergenerational lipid and transgenerational fertility reductions
- Transmission of phenotypes requires repressive histone modifications and argonaute HRDE-1
- Small RNAs transmit hypoxia signal to the naive worm descendants
- Labeled dsRNA F44E5.4/5 is transmitted to F1 and displays a subcellular localization

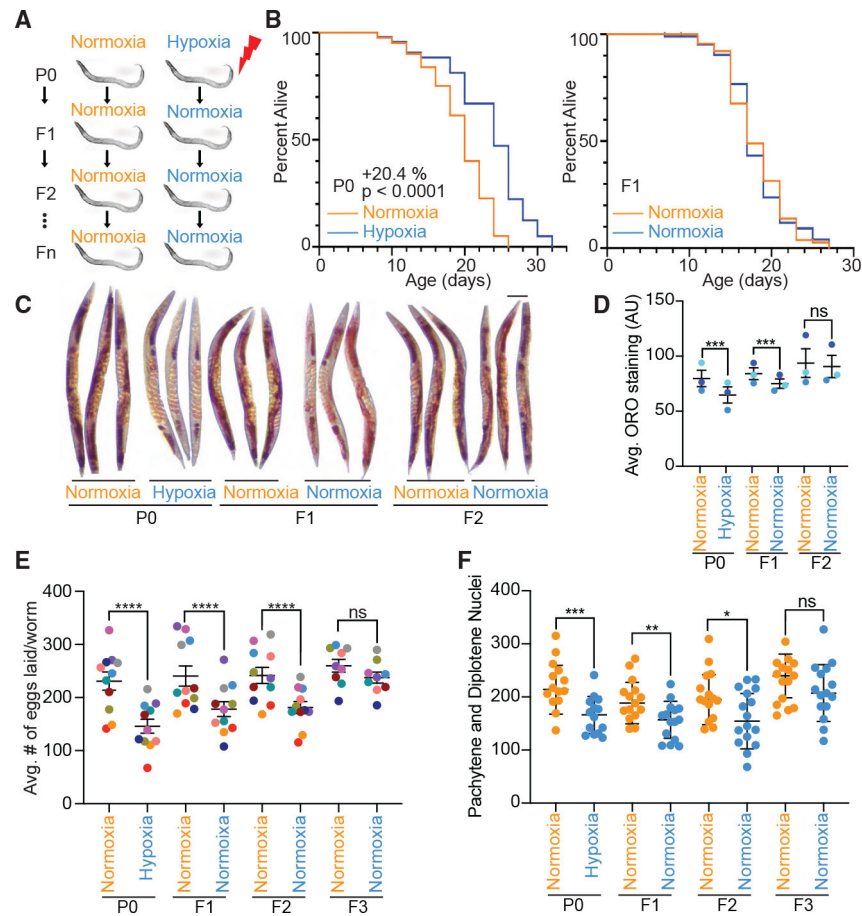


**Figure 1. Hypoxia induces intergenerational lipid reduction and transgenerational fertility reduction in *C. elegans***

(A) Scheme for transgenerational hypoxia in *C. elegans*. Parental (P0) generation is exposed to 0.1% O<sub>2</sub> for 16 h at the L4 stage before being returned to normoxia for subsequent generations.

(B) Hypoxia extends the lifespan in the parental (P0) generation ( $p < 0.0001$ ), but not in naive normoxia-reared progeny (F1) whose ancestors were exposed to hypoxia. Statistics are presented in Table S1.

(C and D) Hypoxia induces an intergenerational lipid reduction as assessed by oil red O staining.

(C) Representative images of young adult *C. elegans*. P0 generation was visualized 24 h after exposure and return to normoxia conditions. Scale bar, 10  $\mu$ m. (D) Quantification of oil red O staining reveals intergenerational decrease in lipid content. Each color-coded dot represents an individual experiment performed in triplicate with ~30 worms, and each column represents the mean  $\pm$  SEM. \*\*\* $p < 0.001$ , as assessed by Fisher's combined probability test.

(E) Hypoxia causes a transgenerational fertility defect in the P0, F1, and F2 generations. Each column represents the mean  $\pm$  SEM of 9–11 independent experiments. Each color-coded dot represents an individual experiment performed in triplicate with ~10 worms per plate. \*\*\* $p < 0.0001$ , <sup>ns</sup> $p > 0.05$ , as assessed by Fisher's combined probability test.



(F) Hypoxia reduces the number of pachytene and diplotene nuclei in the germline of P0 hypoxia-treated and F1 and F2 naive normoxia-reared descendants. Each column represents the mean  $\pm$  SD of ~13–15 worms. \* $p < 0.05$ , \*\* $p < 0.01$ , \*\*\* $p < 0.001$ , <sup>ns</sup> $p > 0.05$ , as assessed by unpaired t test.

ns, not significant. See also Figure S1 and Table S1.

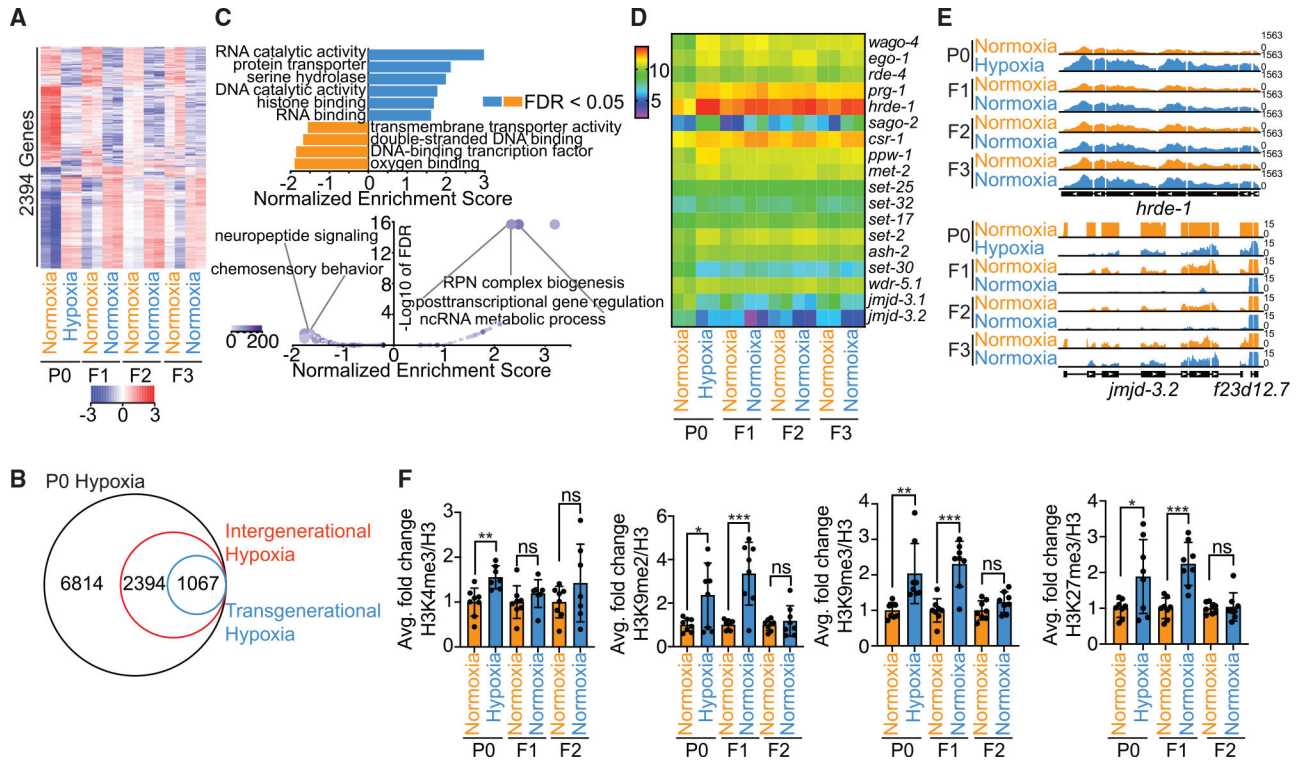


**Figure 2. Hypoxia elicits intergenerational and transgenerational effects on gene expression and histone methylation in naive normoxia-reared descendants**

(A) A subset of transcripts is intergenerationally and transgenerationally misregulated in response to parental hypoxia exposure. The heatmap displays the  $\log_2$ CPM (counts per million) of expected counts of each sample across generations. A list of dysregulated genes is in Table S2.

(B) Venn diagram reveals the subsets of dysregulated genes in response to parental P0 hypoxia exposure that are intergenerationally (F1) dysregulated or transgenerationally (F2) dysregulated despite being reared in normoxia conditions.

(C) Gene Ontology analysis of heritably dysregulated genes reveals upregulation of RNA and histone-binding genes, downregulation of oxygen-binding and chemosensory behavior genes, and false discovery rate (FDR)  $<0.05$  for both upper and lower panels as assessed by Benjamini-Hochberg multiple testing adjustment.

(D) Heatmap focused on transgenerational expression of genes involved in small RNA regulation and chromatin regulation reveals intergenerationally and transgenerationally misregulated enzymes. The values are normalized with  $\log(\text{CPM}+1)$  and represented as fold change between hypoxia and normoxia within each generation.

(E) Genome browser snapshots reveal transgenerational increase in *hrde-1* expression and transgenerational decrease in *jmj3.2* expression in response to parental hypoxia exposure.

(F) Histone methylation of H3K4me3, H3K9me2, H3K9me3, and H3K27me3 increases in response to hypoxia in the parental generation or intergenerationally as assessed by quantification of three independent western blotting experiments performed in triplicate biological replicates. Each column represents the mean  $\pm$  SEM.

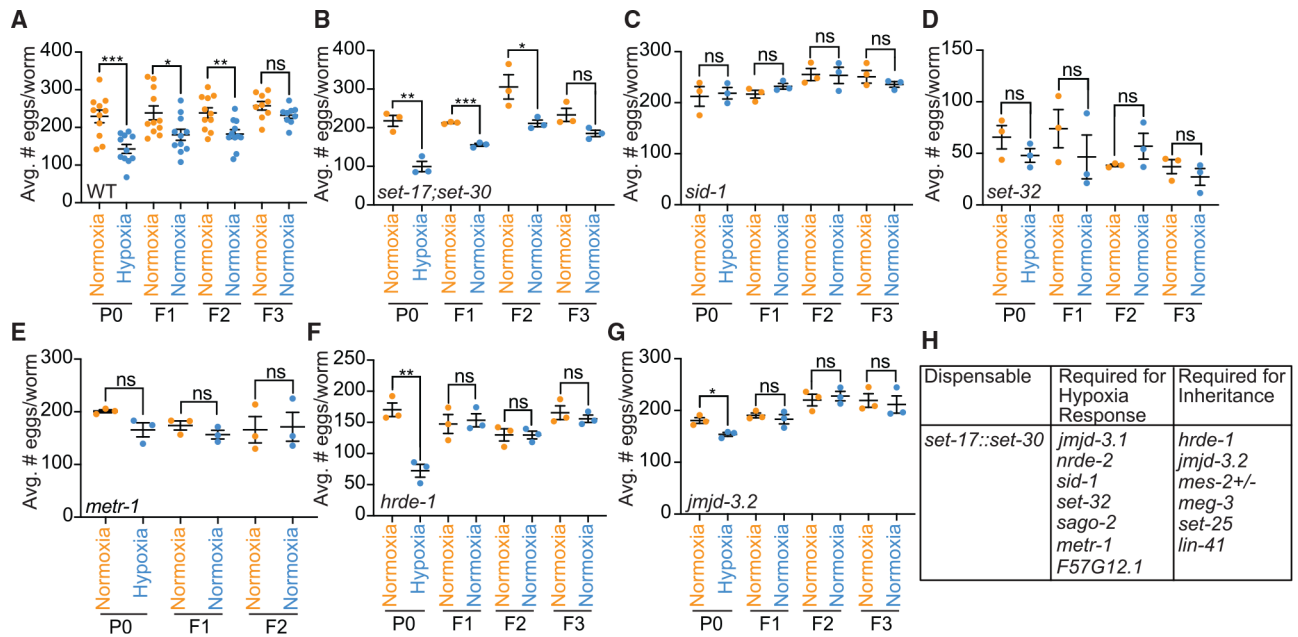
\*p < 0.05, \*\*p < 0.01, \*\*\*p < 0.001, <sup>ns</sup>p > 0.05, as assessed by unpaired t test.  
Representative western blots for one experiment are displayed in Figure S2G. See also  
Figure S2 and Table S2.

Author Manuscript

Author Manuscript

Author Manuscript

Author Manuscript





(D) Transmission of dysregulation of 22G-RNAs in response to parental hypoxia is dependent on *hrde-1*, as represented by heatmap of heritably dysregulated 22G-RNAs across generations in WT and *hrde-1* mutant worms.

(E and F) Venn diagrams display heritable upregulated genes are enriched for *csr-1*-bound targets (E), whereas heritably downregulated genes are enriched for *hrde-1*-bound targets (F).

(G) Dysregulations of 22G-RNAs and their target mRNAs induced by hypoxia are dependent on *hrde-1*. This scatterplot represents the  $\log_2$  fold change of hypoxia relative to normoxia of 22G-RNAs and their target mRNAs (each represented by a single dot) in WT worms (green dots) and *hrde-1* mutant worms (purple dots). Targets are further subdivided based on whether they have been reported to bind to CSR-1 (circles) or the worm-specific argonautes (*wago*) (triangles).

(H) Kernel density plot of 22G-RNAs reveals a small subset of 22G-RNAs continue to display transgenerational dysregulation in response to parental hypoxia and that 22G-RNA dysregulation is dependent on *hrde-1*.

(I) *F44E5.4/5* shows a *hrde-1*-dependent decrease in gene expression in response to parental hypoxia, whereas endogenous siRNAs directed against *F44E5.4/5* show an increase in expression in response to parental hypoxia. This is a representative genome browser snapshot of RNA-seq and small RNA-seq to display the reciprocal relationship between 22G-RNAs and target mRNAs and the *hrde-1* dependency of these RNAs. See also Figure S4.

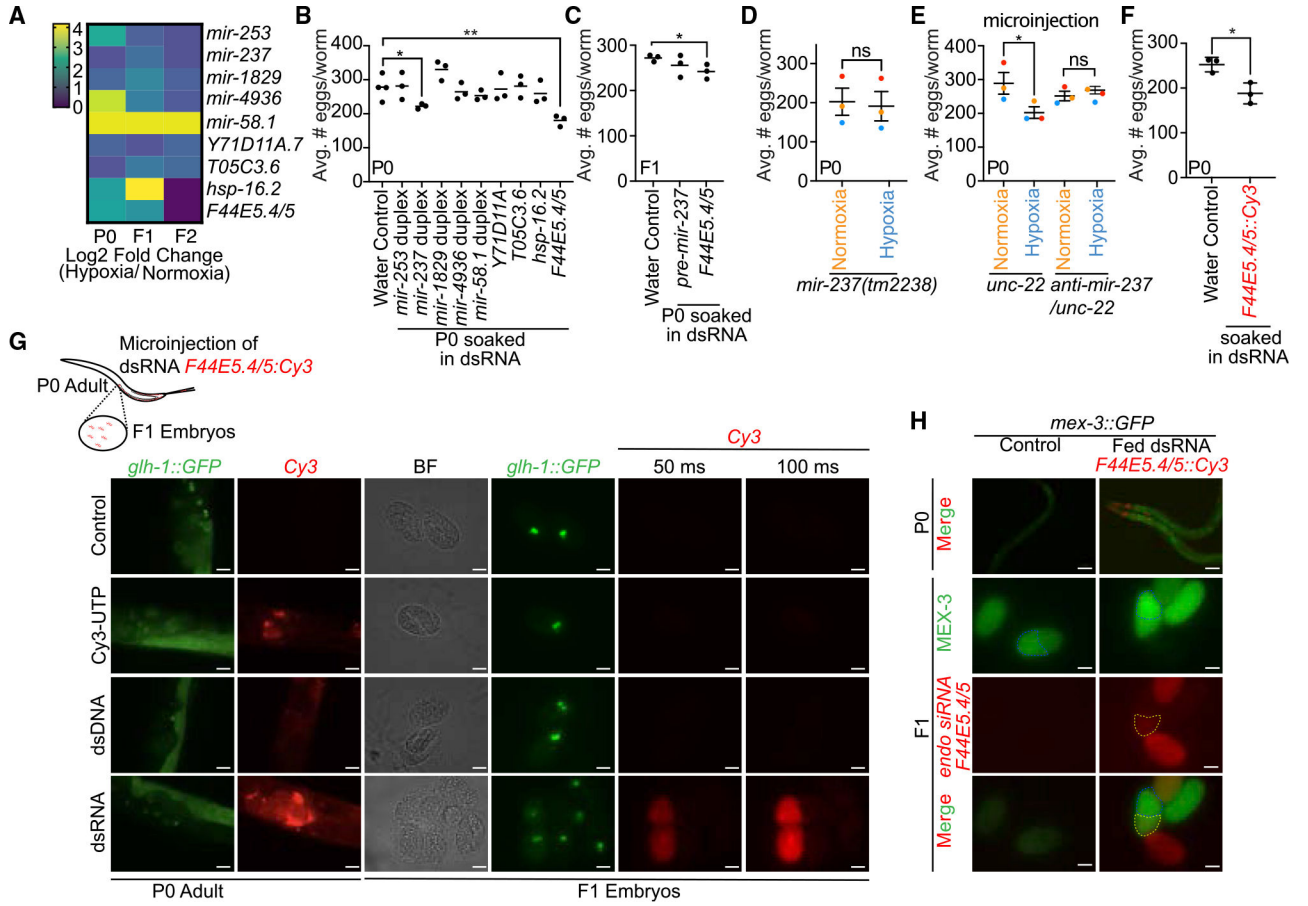


**Figure 5. *F44E5.4/5* dsRNA is sufficient to induce a heritable fertility defect and is transmitted from parents to progeny**

(A) A heatmap displays the relative dysregulation of a subset of small RNAs across generations in response to parental hypoxia.

(B) Soaking naive normoxia-reared worms in dsRNA for *mir-237* and *F44E5.4/5* induces a fertility defect.

(C) The F1 descendants whose parents were soaked in dsRNA directed against *F44E5.4/5* retain a fertility defect. Each dot represents a biological replicate with ~10 worms.

(D and E) *mir-237* is required for the fertility decrease in response to hypoxia as demonstrated by genetic knockout of *mir-237* (D) or antagomir microinjection (E). Each color-coded dot represents an individual experiment performed in triplicate with 10 worms.

\* $p < 0.05$ , \*\* $p < 0.01$ , <sup>ns</sup> $p > 0.05$ , as assessed by unpaired t test. Each column represents the mean  $\pm$  SEM.

(F) Normoxia-reared worms soaked in *in-vitro*-transcribed and cyanine-3-labeled dsRNA *F44E5.4/5* display reduced fertility relative to a water-soaked control. Each dot represents a biological replicate with ~10 worms. Each column represents the mean  $\pm$  SD.

(G) Microinjection of *Cy3*-labeled dsRNA directed against *F44E5.4/5* in *glh-1::GFP* transgenic adults is transmitted to embryos, whereas *Cy3*-UTP or *Cy3*-labeled dsDNA is not transmitted.

(H) Larval stage 4 (L4) *mex-3::GFP* transgenic worms fed *Cy3*-labeled dsRNA directed against *F44E5.4/5* reveal that this specific dsRNA is transmitted to the progeny and is

localized to the anterior side of the embryo. MEX-3 has previously been shown to be a component of P granules and mainly enriched in the posterior side of two-cell embryos.<sup>69</sup>. See also Figure S5.

Author Manuscript

Author Manuscript

Author Manuscript

Author Manuscript



## KEY RESOURCES TABLE

REAGENT or RESOURCE	SOURCE	IDENTIFIER
<b>Antibodies</b>		
rabbit anti-H3	Abcam	Ab1791; RRID:AB_302613
rabbit anti-H3K27me3	Millipore-Sigma	07-449; RRID:AB_310624
rabbit anti-H3K23me3	Active Motif	61500; RRID: AB_2793660
rabbit anti-H3K4me3	Abcam Ab8580	Ab8580; RRID:AB_306649
mouse anti-H3K9me2	Abcam	Ab1220; RRID:AB_449854
rabbit anti-H3K9me3	Abcam	Ab8898; RRID:AB_306848
rabbit anti-H3K4me1	Abcam	Ab8895; RRID:AB_306847
<b>Bacterial and virus strains</b>		
<i>E. coli</i> dam-/dcn-	NEB	C2925
<i>E. coli</i> OP50	Caenorhabditis Genetics Center	OP50
<b>Chemicals, peptides, and recombinant proteins</b>		
Oil red O working solution	Sigma-Aldrich	O1391; CAS:1320-06-5
Immobilon Western Chemiluminescent HRP substrate	Millipore-Sigma	WBKLS0500
Bio-Rad Protein Assay Dye Reagent Concentrate Bradford assay	Bio-Rad	5000006
Cyanine 3-UTP	Enzo Life Sciences	ENZ-42505
RNA 5' Pyrophosphohydrolase (RppH)	NEB	M0356
<b>Critical commercial assays</b>		
mirVana miRNA Isolation kit, with phenol	Life Technologies	AM1560
HiScribe T7 Quick High Yield RNA Synthesis Kit	NEB	E2050
Monarch RNA Cleanup Kit	NEB	T2040
NEXTFLEX Illumina qRNA-Seq Library Prep Kit (Bio Scientific)	Bio Scientific	NOVA-5130-03D
KAPA Library Quantification Kit	Roche Sequencing	KK4824, Cat# 07960140001
Zymo Research R1013 RNAClean & Concentrator-5 with DNase I, Zymo Research	Genesee Scientific	Cat#11-352
NEXTFLEX Small RNA-Seq Kit v3	PerkinElmer	NOVA-5132-06
<b>Deposited data</b>		
Transcriptome and Small RNA analysis of <i>C.elegans</i> from Parental P0 to F3 generations under hypoxic stress in both WT and hrde-1 mutant	GEO	GSE188271
Original unprocessed images	Mendeley Data	<a href="https://doi.org/10.17632/phhyh57zsc.1">https://doi.org/10.17632/phhyh57zsc.1</a>
<b>Experimental models: Organisms/strains</b>		
<i>C. elegans</i> : Strain N2 Bristol	Caenorhabditis Genetics Center	N2

REAGENT or RESOURCE	SOURCE	IDENTIFIER
<i>C. elegans</i> : hrde-1(tm1200)	Caenorhabditis Genetics Center	YY538
<i>C. elegans</i> : hrde-1(gg696[gfp::aid::hrde-1])	Scott Kennedy Lab, Harvard Medical School	YY1714
<i>C. elegans</i> : jmjd-3.1(gk384)	Caenorhabditis Genetics Center	ZR2
<i>C. elegans</i> : jmjd-3.1(gk387) Caenorhabditis Genetics Center	VC912	
<i>C. elegans</i> : jmjd-3.2(tm3121)	Eric Greer Lab, Harvard Medical School	N/A
<i>C. elegans</i> : meg-3(tm4259)	Caenorhabditis Genetics Center	JH3055
<i>C. elegans</i> : mes-2(bn11) unc-4(e120)/mnC1 [dpy-10(e128) unc-52(e444)]	Caenorhabditis Genetics Center	SS186
<i>C. elegans</i> : met-2(ok2307)	Caenorhabditis Genetics Center	RB1789
<i>C. elegans</i> : mir-237(tm2238)	Frank Slack Lab, Harvard Medical School	N/A
<i>C. elegans</i> : nrde-2(gg95)	Caenorhabditis Genetics Center	YY156
<i>C. elegans</i> : sago-2(tm894)	Caenorhabditis Genetics Center	WM154
<i>C. elegans</i> : set-17(n5017)/set-30(gk315)	Eric Greer Lab, Harvard Medical School	N/A
<i>C. elegans</i> : set-25(n5021)	Caenorhabditis Genetics Center	MT17463
<i>C. elegans</i> : set-32(ok1457)	Caenorhabditis Genetics Center	VC967
<i>C. elegans</i> : sid-1(qt9)	Caenorhabditis Genetics Center	HC196
<i>C. elegans</i> : wdr5.1(ok1417)	Caenorhabditis Genetics Center	RB1304
<i>C. elegans</i> : mir-237(tm2238)	Frank Slack Lab, Harvard Medical School	Metheetrairut et al. <sup>78</sup>
<i>C. elegans</i> : meg-3(ax3054[meg-3::meGFP])	Caenorhabditis Genetics Center	JH3503
<i>C. elegans</i> : mex-3(tn1753[gfp::3xflag::mex-3])	Caenorhabditis Genetics Center	DG4269
<i>C. elegans</i> : pgl-1(ax3122[pgl-1::gfp])	Caenorhabditis Genetics Center	JH3269
<i>C. elegans</i> : plk-1(lt18[plk-1::sGFP)::loxp]	Caenorhabditis Genetics Center	OD2425
<i>C. elegans</i> : glh-1(sam24[glh-1::gfp::3xFLAG])I; itIs37[pie-1p::mCherry::H2B::pie-1 3' UTR, unc-119(+)]IV	Dustin Updike Lab (DUP162), MDI Biological Laboratory	Marnik et al. <sup>79</sup>
Oligonucleotides		
cel-miR-237-5p antagomir: UCCUGAGAAUUCUCGAACAGCU	ThermoFisher Scientific	4464084
F44E5.4/5 probe for Northern blot UCGACCUCGGUACUACGUACUC	GeneScript	N/A
Control probe for Northern Blot CGUUAUCCGUACGUACCUGCAC	GeneScript	N/A

REAGENT or RESOURCE	SOURCE	IDENTIFIER
F44E5.4/5 forward primer: CTATCAGAATGGAAAGGTTGAG	Invitrogen	N/A
F44E5.4/5 reverse primer: TCTTCCGTATCTGTGAATGCC	Invitrogen	N/A
Act-1 forward primer: CCAATCCAAGAGAGGTATCCTTAC	Invitrogen	N/A
Act-1 reverse primer: CATTGTAGAAGGTGTGATGCCAG	Invitrogen	N/A
Recombinant DNA		
pLT61 unc-22 RNAi Vector	Addgene	pLT61
Software and algorithms		
ImageJ (1.0)	N/A	<a href="https://imagej.nih.gov/ij/">https://imagej.nih.gov/ij/</a>
StatView 5.0.01	N/A	<a href="https://statview.software.informer.com/5.0/">https://statview.software.informer.com/5.0/</a>
CutAdapt (version 2.5)	N/A	<a href="https://cutadapt.readthedocs.io/en/v2.5/">https://cutadapt.readthedocs.io/en/v2.5/</a>
bowtie2	N/A	<a href="http://bowtie-bio.sourceforge.net/bowtie2/index.shtml">http://bowtie-bio.sourceforge.net/bowtie2/index.shtml</a>
RSEM <sup>80</sup>	Li and Dewey <sup>80</sup>	<a href="https://deweylab.github.io/RSEM/">https://deweylab.github.io/RSEM/</a>
edgeR <sup>81</sup>	Robinson et al. <sup>81</sup>	<a href="https://bioconductor.org/packages/release/bioc/html/edgeR.html">https://bioconductor.org/packages/release/bioc/html/edgeR.html</a>
Shortstack	Axtell et al. <sup>82</sup>	<a href="https://www.shortstack.com">https://www.shortstack.com</a>
featurecount <sup>83</sup>	Liao et al. 2013 <sup>83</sup>	N/A
DEApp <sup>84</sup>	Li and Andrade <sup>84</sup>	N/A
IGV (2.8.2) <sup>79</sup>	Thorvaldsdottir et al. <sup>85</sup>	<a href="https://software.broadinstitute.org/software/igv/2.8.x">https://software.broadinstitute.org/software/igv/2.8.x</a>
Wormcat <sup>86</sup>	Holdorf et al. <sup>86</sup>	<a href="http://www.wormcat.com/">http://www.wormcat.com/</a>
WebGestalt <sup>87</sup>	Zhang et al. <sup>88</sup>	<a href="http://www.webgestalt.org/">http://www.webgestalt.org/</a>
iDEP v0.93beta <sup>89</sup>	Ge et al. <sup>89</sup>	<a href="http://bioinformatics.sdstate.edu/idep/">http://bioinformatics.sdstate.edu/idep/</a>
miRNet <sup>90</sup>	Chang et al. <sup>90</sup>	<a href="https://www.mirnet.ca/">https://www.mirnet.ca/</a>
Prism 9	N/A	<a href="https://www.graphpad.com/scientific-software/prism/">https://www.graphpad.com/scientific-software/prism/</a>
Other		
Eppendorf Galaxy 48R incubator	Sigma-Aldrich	Cat# EPCO48212045
SteREO Discovery V8 microscope	Zeiss	Cat# 495015-0003-000
Fisherbrand Superfrost Plus Microscope slides	Fisher Scientific	Cat# 12-550-15
VECTASHIELD Antifade Mounting Medium with DAPI	Vector Laboratories	Cat# H-1200-10)
Nitrocellulose Membrane	Biorad	Cat #1620097
ChemiDocTouch Imaging System	Biorad	Cat# 1708370
Pellet Pestle Motor	Kimble Kontes	Cat# Z359971
NEXTFLEX Poly (A) Beads 2.0.	Perkin Elmer	Cat# NOVA-512991
Agencourt AmPure XP Magnetic Beads	Beckman Coulter	Cat# A63880